

FEM ANALYSIS OF COMPOSITE PLATES WITH RANDOM MATERIAL PROPERTIES USING MONTE CARLO SIMULATION

A thesis submitted
in partial fulfilment of the requirements
for the degree of

MASTER OF TECHNOLOGY

by

B. NAVANEETHA RAJ



to the

**DEPARTMENT OF AEROSPACE ENGINEERING
INDIAN INSTITUTE OF TECHNOLOGY KANPUR**

February, 1997

FEM ANALYSIS OF COMPOSITE PLATES WITH RANDOM MATERIAL PROPERTIES USING MONTE CARLO SIMULATION

A thesis submitted
in partial fulfilment of the requirements
for the degree of

MASTER OF TECHNOLOGY

by

B. NAVANEETHA RAJ



to the

**DEPARTMENT OF AEROSPACE ENGINEERING
INDIAN INSTITUTE OF TECHNOLOGY KANPUR**

February, 1997

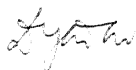
CENTRAL LIBRARY
KANPUR

No. A 123261

AE-1997-M-RAJ-FEM

CERTIFICATE

It is certified that the work contained in the thesis entitled “*FEM analysis of composite plates with random material properties using Monte Carlo simulation*”, by *B. Navaneetha Raj*, has been carried out under our supervision and that this work has not been submitted elsewhere for the award of a degree.



Dr. D. Yadav

Professor

Department of Aerospace Engg.

IIT Kanpur.



Dr. N.G.R. Iyengar

Professor

Department of Aerospace Engg.

IIT Kanpur

ABSTRACT

Composite materials have large number of uncertain parameters associated with its production. It is not possible to control these completely. This results in variations in the properties of composite materials. For accurate modeling, the material properties are considered as random variables. The influence of randomness in material properties on the deflection behaviour of T300/52208 graphite/epoxy composite laminates has been analysed in the present study with the help of Monte Carlo Simulation and FEM. The input material properties in a lot of samples are assumed to vary according to normal distribution and the effect of this is investigated on deflection of plates with different boundary conditions, aspect ratios, end conditions and ply-orientation. The study has also been extended to plates with cut-outs. It has been found that the normalised displacement covariance of the plate reacts to the input randomness in the same way for various aspect ratios, thickness ratios, ply-orientations and support condition. This results in the development of a design curve with which the deflection statistics of a different plates can be predicted with a fair degree of accuracy.

ACKNOWLEDGEMENT

I take this opportunity to thank my thesis supervisors Dr. N.G.R. Iyengar and Dr. D. Yadav, for their inspiration and valuable suggestions in carrying out this work. I consider myself fortunate to have worked under them for the freedom and constant encouragement they gave throughout this work.

Apart from academics I have earned a wealth of friends, they were an inseparable part of my life at IITK. Perusu for “siva siva”, periya vandi for “Mumbai payanam”, chinna vandi for “1996 New Year”, the Shaileshes for “so many things”, joye for “vaay punn ...”, Tats for “gulab jamun”, a special mention of Gondu for “patthu nimisham”, palani for “Maadu”, pandi for “koli samayal”, ramki for “potti yenika”, senthil

And my special thanks to Gomes and Ravi, for all they have done and meant to me.

This work was supported by ARDB structures panel . I am thankful to them.

B. Navaneetha Raj

Contents

Certificate	ii
Abstract	iii
Acknowledgement	iv
1 Introduction	1
2 Formulation for static analysis	6
2.1 Displacement field	6
2.2 Strain-Displacement relations	9
2.3 Stress-Strain relations for an orthotropic lamina	10
2.4 Laminate constituent equations.	11
2.5 Finite element modeling	12
2.6 Strain energy of the laminate	17
2.7 Potential energy of the external load	17
2.8 Total potential	19
3 Solution approach	21
3.1 Input sample generation	21
3.1.1 Number generator	21

3.1.2	Preprocessing of raw data	23
3.2	System analysis	24
3.3	Post processing of the response behavior	25
4	Results and Discussion	26
4.1	Deflection characteristics of rectangular plates	27
4.1.1	Response sensitivity	36
4.1.2	Normalised characteristics of composite plate	38
4.2	Deflection of plates with cut-outs	41
5	Conclusions and scope for future work	49
	References	51

List of Figures

1.1	Development of uncertainty in the material property of laminated composites.	4
2.1	Laminated composite rectangular plate	7
3.1	Lay-out of the code developed	22
3.2	Mesh and Boundary Conditions	25a
4.1	Plate deflection characteristic with σ_{E_t}	29
4.2	Plate deflection characteristic with σ_{E_t}	31
4.3	Plate deflection characteristic with $\sigma_{\nu_{tz}}$	32
4.4	Plate deflection characteristic with $\sigma_{G_{tz}}$ and $\sigma_{G_{tz}}$	34
4.5	Plate deflection characteristic with $\sigma_{G_{tz}}$	35
4.6	Response sensitivity of the composite plate to material properties	37
4.7	Normalised reponse characteristics of rectangular plates	39
4.8	Superimposed plate response characteristics	40
4.9	Characteristics of the composite plate with cut-out, $l/d = 2$	42
4.10	Characteristics of the composite plate with cut-out, $l/d = 4$	43
4.11	Characteristics of the composite plate with cut-out, $l/d = 6$	44
4.12	Characteristics of the composite plate with cut-out, $l/d = 8$	45
4.13	Characteristics of the composite plate with cut-out, $l/d = 10$	46
4.14	Characteristics of the plate with cut-out, $l/d=2$ to 10	48

List of Tables

1.1	Variation of reported stiffness properties for a widely used Graphite/Epoxy system, from five sources (Sources: Major Airframe Company Reports). . .	2
1.2	Variation of reported stiffness properties for a widely used Graphite/Epoxy system, from five sources (Sources: Major Airframe Company Reports). . .	3
3.1	Convergence and Validation Study).	25b

List of Symbols

AR	:	Aspect Ratio of the Plate	(a/b)
CC	:	Clamped - Clamped edge condition	
SS	:	Simply Supported edge condition	
SD	:	Standard Deviation	
RV	:	Random Variable	
a	:	Length of the Plate	(m)
a/h	:	Thickness Ratio of the Plate	
b	:	Breadth of the Plate	(m)
d	:	Diameter of the Cut -out	(m)
$f(r,\theta)$:	Polar Function	
h	:	Thickness of the Plate	(m)
l	:	Larger Dimension of the Plate	(m)
(l,t,z)	:	Material axis of the laminate	
σ	:	Standard Deviation	
μ	:	Mean	

Chapter 1

Introduction

Composite materials are known to have many advantages over conventional materials. Further these allow the designer the flexibility of tailoring them to meet specific needs. This makes composites a contender for the material of the future, which is also evident from the fact that more and more composite materials are replacing conventional materials in engineering and industrial applications. The mechanical and physical properties of the raw materials fiber, resin etc. as provided by the manufacturers are generally average properties subject to specific production conditions. Because of inherent variations in these conditions from time to time a dispersion in the properties of raw materials is always present.

Fiber and resin are combined in a suitable proportions to form a lamina. Factors such as temperature, pressure, moisture, fiber spacing, voids, impurities curing time etc. enter along with the variations in raw material properties. These manifest themselves as the variation in lamina properties. The lamina are stacked together to meet the requirements of the designer to form laminates, the variations in the lamina properties results in variations in the reduced stiffness coefficients of the laminates.

As shown in Fig.1.1 the uncertainty in the material properties gets introduced at various levels through different parameters associated with the composite. Further it is well under-

Table 1.1: Variation of reported stiffness properties for a widely used Graphite/Epoxy system, from five sources (Sources: Major Airframe Company Reports).

Elastic Constants($10^6 psi$)	1	2*	3*	4	5	Max. Diff. %
Long. tensile modulus	20.8	18.1	21	20.6	18.5	16
Long. compr. modulus	18.6	14.5	21	19.8	18.5	45
Trans. tensile. modulus	1.9	1.8	1.7	1.3	1.6	46
In-plane shear modulus	0.85	-	0.65	0.8	0.65	31
Poisson's ratio	0.30	-	-	0.32	0.25	28

*-Different divisions of the same company

stood that it is not possible to control all the parameters involved in the manufacturing of composites. Tables 1.1 and 1.2 [1] illustrate the variation in strength and stiffness properties of composite laminates, observed in a molding lot. The variations in the strength and stiffness properties introduces a factor of uncertainty in the behavior of structures made up of the composite materials. Accurate predictions of the system behavior of composites in the presence of the uncertainties favors a probabilistic analysis approach for composites by modeling their properties as random variables(RVs).

The uncertainty in the material strength and stiffness of composites has caught the attention of researchers. Ibrahim [2] reviewed a number of topics pertaining to structural dynamics with parameter uncertainties. Nakagiri *et al.* [3] have studied simply supported(SS) graphite/epoxy plates with Stochastic Finite Element Method (SFEM) taking fiber orientation, layer thickness and layer number as random variables, and found that the overall stiffness of FRP laminated plates is found out to be largely dependant on fiber orientation. Leissa and Martin [4] have analyzed the vibration and buckling of rectangular composite plates, and have established that variation in fiber spacing or redistribution of fibers tend to increase the buckling load by 38 percent and the fundamental frequency by 21 percent. Englestad and Reddy [5] have studied metal matrix composites (MMC) based

Table 1.2: Variation of reported stiffness properties for a widely used Graphite/Epoxy system, from five sources (Sources: Major Airframe Company Reports).

Strength Properties($10^3 psi$)	1	2*	3*	4	5	Max. Diff. %
Long. tension	274	190	180	164	169	67
Long. compression	280	126	180	126	162	122
Trans. tension	9.5	5.2	8.0	5.4	6.0	83
Trans compression	39	-	30	21	25	86
In-plane shear	17.3	-	12	8.4	-	106
Interlaminar shear	-	13.5	13	-	7.1	90

*-Different divisions of the same company

on probabilistic micromechanics nonlinear analysis procedure of MMC. They have used Monte Carlo Simulation (MCS), and different probabilistic distributions to incorporate the uncertainty of constituent level properties. Roy and de Wilde in first part of their work [6] have established a procedure to obtain the best fit for each material property. Further they have studied the behavior of perforated plate and determined the probability distribution of the response. The input variables have been simulated using MCS and SFEM has been used for the analysis. Salim *et. al* [7, 8, 9] studied the statistical response of the system considering the material properties such as longitudinal modulus, Poisson's ratio, transverse elastic modulus, etc., as independant random variables on $[90^0/0^0/90^0]$ and $[0^0]$, rectangular, SS and clamped(CC) plates subject to static loads. Salim *et al*[9] have shown that there is change in the rate and the order of the natural frequency with SD of input RV and change in boundary condition of the plate.

One can see that the uncertainty in composite material properties enters at the raw materials level [4, 5]. In references [1, 3, 6] and [7] the dispersion in the behavior of composite structure is assumed to be due to the variation in lamina properties. These studies also takes care of the variation in the properties of the raw materials. Salim *et al*[7] used the

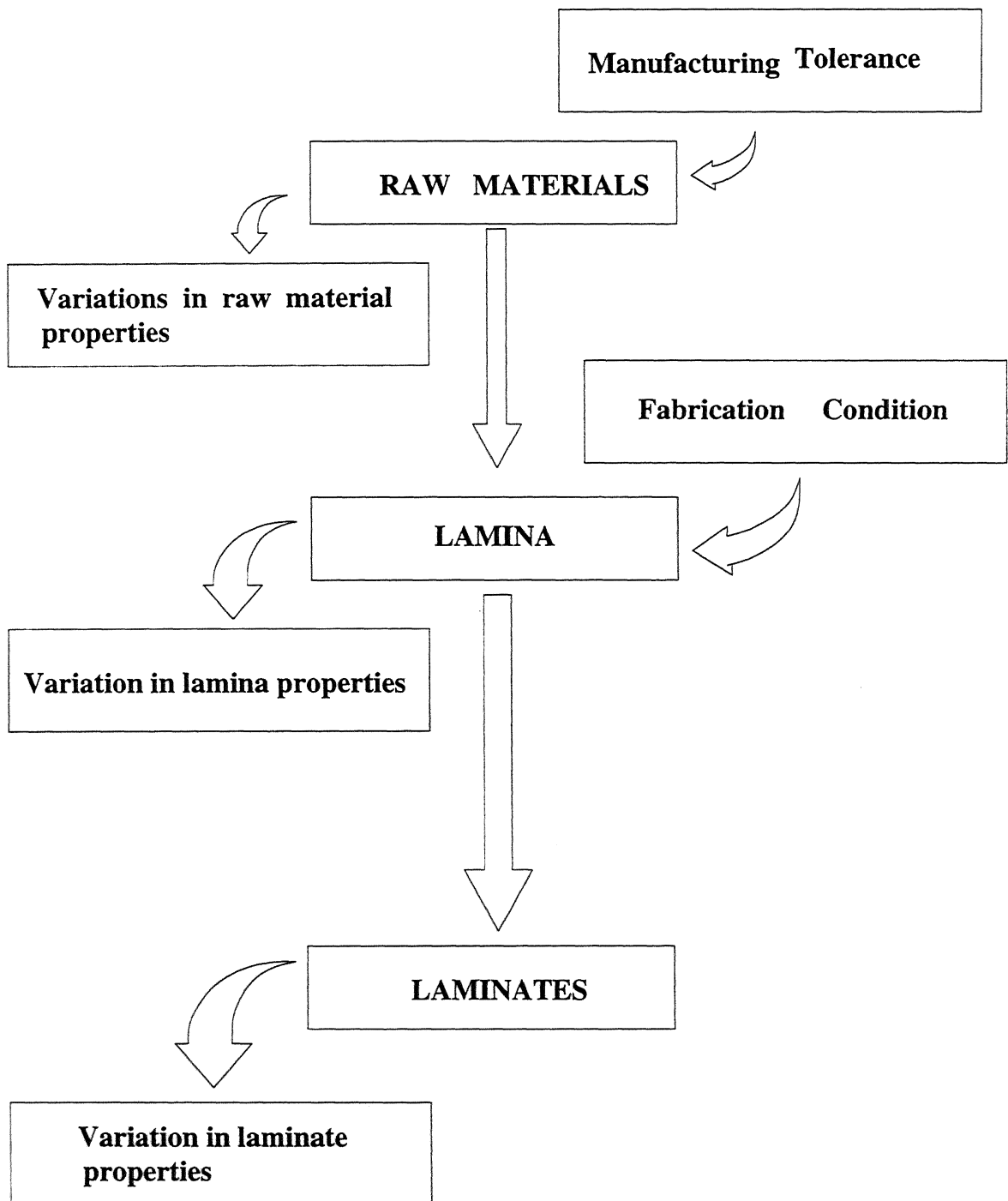


Figure 1.1: Development of uncertainty in the material property of laminated composites.

perturbation technique with Rayleigh-Ritz formulation to analyse the bending, buckling and vibration of composite plates. With the Rayleigh-Ritz method, different formulations are needed to handle different problems. That is the formulations have to be changed for different end conditions, different loadings, etc. This problem can be overcome by using FEM for deflection analysis. The perturbation technique though gives acceptable results, the method fails for larger dispersions in the input random variables. The SFEM method can handle larger uncertainties in the input parameters. However, it is computationally expensive and being a specialised technique its other applications are limited. This has motivated the use of a conventional FEM in the present study. Though this method is also computationally intensive, the analysis can be done with commercially available FEM modules. Most of the earlier studies have been performed where material properties vary independently. In a practical problem the material properties vary randomly and simultaneously. The present study attempts to cover this aspect also.

The variation in the properties are present in a given lot of plates as well as there are variation of the individual properties over the domain of the plate. The present study focusses on the variation in the lot, variation in property in a given lot which is assumed to conform with the normal distribution. In the present study the stiffness properties of lamina such as E_l , E_t , ν_{lt} , G_{lt} , G_{tz} and G_{lz} are considered to be the basic random variables. Deflection is one of the important behavioral parameters of a structure and this may be a constraint on the design for certain applications. In the present analysis the bending of composite laminates due to external loading has been studied with the above mentioned material properties modelled as random variables. Effect of the dispersion in the input material properties is studied on the flexural response of the plate. MCS with FEM is adopted to obtain the deflection response of the laminated plates and its statistics with different input characteristics and cut out shapes.

Chapter 2

Formulation for static analysis

In this section, the details of finite element analysis for plate bending is being presented. A suitable displacement model is adopted and from these the strain displacement relations are developed. Since this study is concerned with composite plates, the stress-strain relationship for an orthotropic lamina is presented. These are utilized to obtain the laminate constituent equation. Finally the governing equation for the flexural response of laminated anisotropic plates is presented.

2.1 Displacement field

The rectangular laminated plate analyzed is represented in Fig.2.1. u , v and w are the displacements along x , y and z axes respectively. u_0 , v_0 and w_0 represent the mid-plane displacements, ψ_x and ψ_y are the rotations. Thus the nodal displacements model has five degree of freedom namely, u_0 , v_0 , w_0 , ψ_x , ψ_y .

A displacement field of the following form is used for the present study.

$$\begin{aligned}u(x, y, z) &= u_0(x, y) + f_1(z)\psi_x(x, y) + f_2(z)\partial w_0/\partial x \\v(x, y, z) &= v_0(x, y) + f_1(z)\psi_y(x, y) + f_2(z)\partial w_0/\partial y \\w(x, y, z) &= w_0(x, y)\end{aligned}\tag{2.1}$$

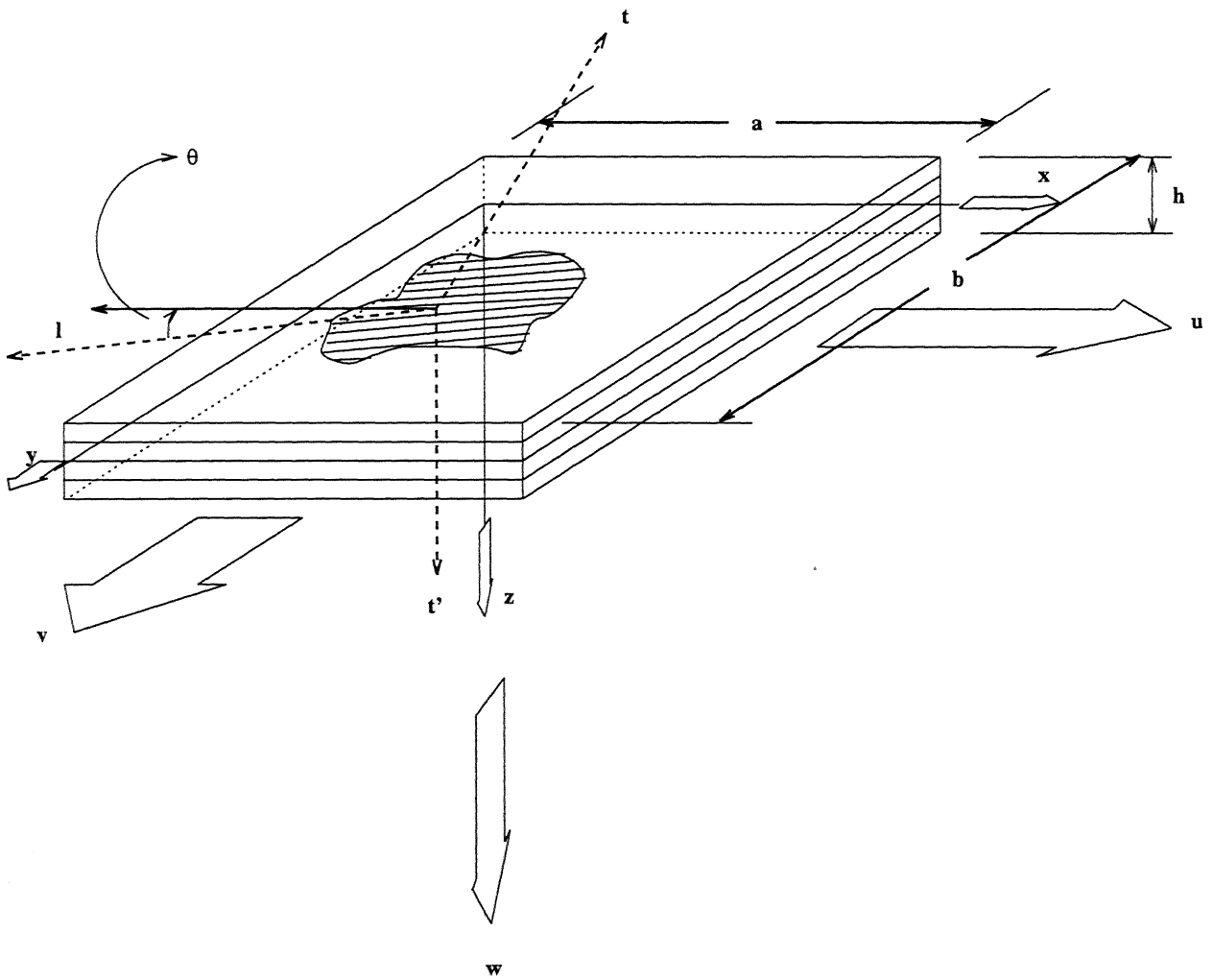


Figure 2.1: Laminated composite rectangular plate

where,

$$\begin{aligned} f_1(z) &= C_1 z - C_2 z^3 \\ f_2(z) &= -C_4 z^3 \end{aligned} \quad (2.2)$$

The displacement field can be transformed either to first order shear deformation theory (FSDT) model [10] or higher order shear deformation theory (HSDT) model by changing the values of the constants C_1 , C_2 and C_4 [11, 12].

with,

$$\begin{aligned} C_1 &= 1; C_2 = C_4 = 0 \text{ for FSDT model} \\ C_1 &= 1; C_2 = C_4 = -\frac{4}{3h^2} \text{ for HSDT model} \end{aligned} \quad (2.3)$$

In the displacement model given above, u and v are dependent on the derivative of the out of plane displacement w . The strain vector would have a second order derivative of the out of plane displacement hence for the FEM analysis its necessary to employ an element with a C^1 continuity. To overcome the complexity and difficulty involved with making a choice of C^1 continuity element, the derivative of the out of plane displacement are themselves considered as separate DOFs θ_x , θ_y . Thus the 5 DOF with C^1 continuity is transformed into a 7 DOF C^0 continuity.

Thus the displacement model adopted in the present study is given by the following :

$$\begin{aligned} u(x, y, z) &= u_0(x, y) + f_1(z)\psi_x(x, y) + f_2(z)\theta_x(x, y) \\ v(x, y, z) &= v_0(x, y) + f_1(z)\psi_y(x, y) + f_2(z)\theta_y(x, y) \\ w(x, y, z) &= w_0(x, y) \end{aligned} \quad (2.4)$$

where, $\theta_x = \partial w_0 / \partial x$ and $\theta_y = \partial w_0 / \partial y$.

2.2 Strain-Displacement relations

The strain displacement relations are obtained using small deformation theory [13].

$$\begin{aligned}\{\epsilon_b\} &= \begin{Bmatrix} \epsilon_x \\ \epsilon_y \\ \gamma_{xy} \end{Bmatrix} = \{\epsilon_1\} + z\{\kappa_1\} + z^3\{\kappa_2\} \\ \{\epsilon_s\} &= \begin{Bmatrix} \gamma_{yz} \\ \gamma_{xz} \end{Bmatrix} = \{\epsilon_2\} + z^2\{\kappa_3\}\end{aligned}\quad (2.5)$$

where, ϵ_b is the bending strain vector and ϵ_s being the shear strain vector.

Where,

$$\begin{aligned}\{\epsilon_1\} &= \begin{Bmatrix} \epsilon_{11} \\ \epsilon_{21} \\ \epsilon_{61} \end{Bmatrix} = \begin{Bmatrix} u_{0,x} \\ v_{0,y} \\ u_{0,y} + v_{0,x} \end{Bmatrix} \\ \{\epsilon_2\} &= \begin{Bmatrix} \epsilon_{41} \\ \epsilon_{51} \end{Bmatrix} = C_1 \begin{Bmatrix} \psi_y \\ \psi_x \end{Bmatrix} + \begin{Bmatrix} w_{0,y} \\ w_{0,x} \end{Bmatrix} \\ \{\kappa_1\} &= \begin{Bmatrix} \kappa_{11} \\ \kappa_{21} \\ \kappa_{61} \end{Bmatrix} = C_1 \begin{Bmatrix} \psi_{x,x} \\ \psi_{y,y} \\ \psi_{x,y} + \psi_{y,x} \end{Bmatrix} \\ \{\kappa_2\} &= \begin{Bmatrix} \kappa_{12} \\ \kappa_{22} \\ \kappa_{62} \end{Bmatrix} = -C_2 \begin{Bmatrix} \psi_{x,x} \\ \psi_{y,y} \\ \psi_{x,y} + \psi_{y,x} \end{Bmatrix} - C_4 \begin{Bmatrix} \theta_{x,x} \\ \theta_{y,y} \\ \theta_{x,y} + \theta_{y,x} \end{Bmatrix} \\ \{\kappa_3\} &= \begin{Bmatrix} \kappa_{41} \\ \kappa_{51} \end{Bmatrix} = -3C_2 \begin{Bmatrix} \psi_y \\ \psi_x \end{Bmatrix} - C_4 \begin{Bmatrix} \theta_y \\ \theta_x \end{Bmatrix}\end{aligned}\quad (2.6)$$

2.3 Stress-Strain relations for an orthotropic lamina

The constituent equation for k^{th} lamina of the laminate can be written as [13]

$$\begin{Bmatrix} \sigma_l \\ \sigma_t \\ \tau_{lt} \\ \tau_{tz} \\ \tau_{lz} \end{Bmatrix}^k = \begin{bmatrix} Q_{11} & Q_{12} & 0 & 0 & 0 \\ Q_{12} & Q_{22} & 0 & 0 & 0 \\ 0 & 0 & Q_{66} & 0 & 0 \\ 0 & 0 & 0 & Q_{44} & 0 \\ 0 & 0 & 0 & 0 & Q_{55} \end{bmatrix}^k \begin{Bmatrix} \epsilon_l \\ \epsilon_t \\ \gamma_{lt} \\ \gamma_{tz} \\ \gamma_{lz} \end{Bmatrix}^k \quad (2.7)$$

where 'l' and 't' represent longitudinal and transverse directions and $[Q_{ij}]$ s are the stiffness coefficients of the lamina. These are related to matrix properties as follows:

$$\begin{aligned} Q_{11} &= E_l / (1 - \nu_{lt}\nu_{tl}) \\ Q_{22} &= E_t / (1 - \nu_{lt}\nu_{tl}) \\ Q_{12} &= \nu_{lt}E_t / (1 - \nu_{lt}\nu_{tl}) \\ Q_{66} &= G_{lt} \\ Q_{44} &= G_{tz} \\ Q_{55} &= G_{lz} \end{aligned} \quad (2.8)$$

The transformed stress-strain relations with respect to laminate co-ordinate system are,

$$\begin{Bmatrix} \sigma_x \\ \sigma_y \\ \tau_{xy} \\ \tau_{yz} \\ \tau_{xz} \end{Bmatrix}^{(k)} = \begin{bmatrix} \bar{Q}_{11} & \bar{Q}_{12} & \bar{Q}_{16} & 0 & 0 \\ \bar{Q}_{12} & \bar{Q}_{22} & \bar{Q}_{26} & 0 & 0 \\ \bar{Q}_{16} & \bar{Q}_{26} & \bar{Q}_{66} & 0 & 0 \\ 0 & 0 & 0 & \bar{Q}_{44} & \bar{Q}_{45} \\ 0 & 0 & 0 & \bar{Q}_{45} & \bar{Q}_{55} \end{bmatrix}^{(k)} \begin{Bmatrix} \epsilon_x \\ \epsilon_y \\ \gamma_{xy} \\ \gamma_{yz} \\ \gamma_{xz} \end{Bmatrix}^{(k)} \quad (2.9)$$

Here $[\bar{Q}_{ij}]$ are the transformed reduced stiffness coefficients for the κ_{th} lamina.

$$\begin{aligned}
\bar{Q}_{11} &= Q_{11}C^4 + 2(Q_{12} + 2Q_{66})C^2S^2 + Q_{22}S^4 \\
\bar{Q}_{22} &= Q_{11}S^4 + 2(Q_{12} + 2Q_{66})C^2S^2 + Q_{22}C^4 \\
\bar{Q}_{12} &= (Q_{11} + Q_{12} - 4Q_{66})C^2S^2 + Q_{12}(C^4 + S^4) \\
\bar{Q}_{16} &= (Q_{11} - Q_{12} - 2Q_{66})C^3S + (Q_{12} - Q_{22} + 2Q_{66})CS^3 \\
\bar{Q}_{26} &= (Q_{11} - Q_{12} - 2Q_{66})CS^3 + (Q_{12} - Q_{22} + 2Q_{66})SC^3 \\
\bar{Q}_{66} &= (Q_{11} + Q_{22} - 2Q_{12} - 2Q_{66})C^2S^2 + Q_{66}(S^4 + C^4) \\
\bar{Q}_{44} &= Q_{44}C^2 + Q_{55}S^2 \\
\bar{Q}_{55} &= Q_{44}S^2 + Q_{55}C^2 \\
\bar{Q}_{45} &= (Q_{44} - Q_{55})CS
\end{aligned} \tag{2.10}$$

where $C = \cos \theta$ and $S = \sin \theta$.

2.4 Laminate constituent equations.

The stress and strains are function of all the three co-ordinates x , y and z respectively. To reduce the complexity of the number of dimensions, statically equivalent force and moment system or the concept of stress resultants is used. These are obtained by integrating the respective stresses along the laminate thickness direction [13].

$$\begin{aligned}
\begin{Bmatrix} N_x & M_x & P_x \\ N_y & M_y & P_y \\ N_{xy} & M_{xy} & P_{xy} \end{Bmatrix} &= \sum_{k=1}^{NL} \int_{Z_{k-1}}^{Z_k} \begin{Bmatrix} \sigma_x \\ \sigma_y \\ \tau_{xy} \end{Bmatrix}^{(k)} (1, Z, Z^3) dZ \\
\begin{Bmatrix} Q_y & R_y \\ Q_x & R_x \end{Bmatrix} &= \sum_{k=1}^{NL} \int_{Z_{k-1}}^{Z_k} \begin{Bmatrix} \tau_{yz} \\ \tau_{xz} \end{Bmatrix}^{(k)} (1, Z^2) dZ
\end{aligned} \tag{2.11}$$

Where, NL gives the number of layers and the resultant force and moment equation can be written as: $\{N\} = [D]\{\bar{\epsilon}\}$

where, $\{N\} = \{ N_x N_y N_{xy} M_x M_y M_{xy} P_x P_y P_{xy} Q_y Q_x R_y R_x \}$

and $\{\bar{\epsilon}\} = \{ \epsilon_{11} \epsilon_{21} \epsilon_{61} \kappa_{11} \kappa_{21} \kappa_{61} \kappa_{12} \kappa_{22} \kappa_{62} \epsilon_{41} \epsilon_{51} \kappa_{41} \kappa_{51} \}$

where $\dots \{P_x P_y P_{xy}\}$ and $\{R_y R_x\}$ are higher order moments and shear stress resultants, and,

$$[D] = \begin{bmatrix} [A1] & [B] & [E] & 0 & 0 \\ [B] & [D1] & [F1] & 0 & 0 \\ [E] & [F1] & [H] & 0 & 0 \\ 0 & 0 & 0 & [A2] & [D2] \\ 0 & 0 & 0 & [D2] & [F2] \end{bmatrix} \quad (2.12)$$

The plate stiffness matrices $A1_{ij}$, $A2_{ij}$, B_{ij} , \dots H_{ij} are given by,

$$(A1_{ij} \ B_{ij} \ D1_{ij} \ E_{ij} \ F1_{ij} \ H_{ij}) = \sum_{k=1}^{NL} \int_{Z_{k-1}}^{Z_k} \bar{Q}_{ij}^{(k)}(1, Z, Z^2, Z^3, Z^4, Z^6) dZ, i, j = 1, 2, 6$$

$$(A2_{ij} \ D2_{ij} \ F2_{ij}) = \sum_{k=1}^{NL} \int_{Z_{k-1}}^{Z_k} \bar{Q}_{ij}^{(k)}(1, Z^2, Z^4) dZ, i, j = 4, 5 \quad (2.13)$$

2.5 Finite element modeling

The displacement model can be represented concisely by the following:

$$\{\underline{u}\} = [\bar{N}]\{\delta\} \quad (2.14)$$

where, $()'$ refers to transpose of the vector/matrix.

$$\{\underline{u}\} = \{u \ v \ w\}' \quad (2.15)$$

$$[\bar{N}] = \begin{bmatrix} 1 & 0 & 0 & 0 & f_2(z) & 0 & f_1(z) \\ 0 & 1 & 0 & f_2(z) & 0 & f_1(z) & 0 \\ 0 & 0 & 1 & 0 & 0 & 0 & 0 \end{bmatrix} \quad (2.16)$$

$$\{\delta\} = \{u_0 \ v_0 \ w_0 \ \theta_y \ \theta_x \ \psi_y \ \psi_x\}' \quad (2.17)$$

$\{\delta\}$ is the ' displacement vector '. An isoparametric element is employed for the finite element modeling. For this type of element the displacement vector and the geometry are represented by the same interpolating functions.

$$\{\delta\} = \sum_{i=1}^{NN} N_i \{\delta_i\} \quad (2.18)$$

$$x = \sum_{i=1}^{NN} N_i x_i \quad (2.19)$$

$$y = \sum_{i=1}^{NN} N_i y_i \quad (2.20)$$

Here NN is the number of nodes per element. N_i is the shape function for the i_{th} node and $\{\delta_i\}$ is the displacement vector for the i_{th} node. The shape function depends on the type of element employed. The shape functions for a nine noded isoparametric Lagrangian element is given below

$$\begin{aligned} N_1 &= \frac{1}{4}\xi(1-\xi)\eta(1-\eta) \\ N_2 &= -\frac{1}{2}(1-\xi^2)\eta(1-\eta) \\ N_3 &= -\frac{1}{4}\xi(1+\xi)\eta(1-\eta) \\ N_4 &= -\frac{1}{2}\xi(1-\xi)(1-\eta^2) \\ N_5 &= (1-\xi^2)(1-\eta^2) \\ N_6 &= \frac{1}{2}\xi(1+\xi)(1-\eta^2) \\ N_7 &= -\frac{1}{4}\xi(1-\xi)\eta(1+\eta) \\ N_8 &= \frac{1}{2}(1-\xi^2)\eta(1+\eta) \\ N_9 &= \frac{1}{4}\xi(1+\xi)\eta(1+\eta) \end{aligned} \quad (2.21)$$

The strain vectors given in Equation 2.5 and 2.11 may be written as,

$$\begin{aligned}
 \{\epsilon_1\} &= [L_1]\{\delta\} \\
 \{\epsilon_2\} &= [L_2]\{\delta\} \\
 \{\kappa_1\} &= [L_3]\{\delta\} \\
 \{\kappa_2\} &= [L_4]\{\delta\} \\
 \{\kappa_3\} &= [L_5]\{\delta\} \\
 \text{and } \{\bar{\epsilon}\} &= [\mathcal{L}]\{\delta\}
 \end{aligned} \tag{2.22}$$

In the above equations, $[L_1], \dots [L_5]$ and $[\mathcal{L}]$ are matrices of differential operators

$$\begin{aligned}
 [L_1] &= \begin{bmatrix} \frac{\partial}{\partial x} & 0 & 0 & 0 & 0 & 0 & 0 \\ 0 & \frac{\partial}{\partial y} & 0 & 0 & 0 & 0 & 0 \\ \frac{\partial}{\partial y} & \frac{\partial}{\partial x} & 0 & 0 & 0 & 0 & 0 \end{bmatrix} \\
 [L_2] &= \begin{bmatrix} 0 & 0 & \frac{\partial}{\partial y} & 0 & 0 & C_1 & 0 \\ 0 & 0 & \frac{\partial}{\partial x} & 0 & 0 & 0 & C_1 \end{bmatrix} \\
 [L_3] &= \begin{bmatrix} 0 & 0 & 0 & 0 & 0 & 0 & C_1 \frac{\partial}{\partial x} \\ 0 & 0 & 0 & 0 & 0 & C_1 \frac{\partial}{\partial y} & 0 \\ 0 & 0 & 0 & 0 & 0 & C_1 \frac{\partial}{\partial x} & C_1 \frac{\partial}{\partial y} \end{bmatrix} \\
 [L_4] &= - \begin{bmatrix} 0 & 0 & 0 & 0 & C_4 \frac{\partial}{\partial x} & 0 & C_2 \frac{\partial}{\partial x} \\ 0 & 0 & 0 & C_4 \frac{\partial}{\partial y} & 0 & C_2 \frac{\partial}{\partial y} & 0 \\ 0 & 0 & 0 & C_4 \frac{\partial}{\partial x} & C_4 \frac{\partial}{\partial y} & C_2 \frac{\partial}{\partial x} & C_2 \frac{\partial}{\partial y} \end{bmatrix} \\
 [L_5] &= -3 \begin{bmatrix} 0 & 0 & 0 & C_4 & 0 & C_2 & 0 \\ 0 & 0 & 0 & 0 & C_4 & 0 & C_2 \end{bmatrix}
 \end{aligned} \tag{2.23}$$

The assembled differential operator is written as:

$$[\mathcal{L}] = \begin{bmatrix} \frac{\partial}{\partial x} & 0 & 0 & 0 & 0 & 0 & 0 \\ 0 & \frac{\partial}{\partial y} & 0 & 0 & 0 & 0 & 0 \\ \frac{\partial}{\partial y} & \frac{\partial}{\partial x} & 0 & 0 & 0 & 0 & 0 \\ 0 & 0 & 0 & 0 & 0 & 0 & C_1 \frac{\partial}{\partial x} \\ 0 & 0 & 0 & 0 & 0 & C_1 \frac{\partial}{\partial y} & 0 \\ 0 & 0 & 0 & 0 & 0 & C_1 \frac{\partial}{\partial x} & C_1 \frac{\partial}{\partial y} \\ 0 & 0 & 0 & 0 & -C_4 \frac{\partial}{\partial x} & 0 & -C_2 \frac{\partial}{\partial x} \\ 0 & 0 & 0 & -C_4 \frac{\partial}{\partial y} & 0 & -C_2 \frac{\partial}{\partial y} & 0 \\ 0 & 0 & 0 & -C_4 \frac{\partial}{\partial x} & -C_4 \frac{\partial}{\partial y} & -C_2 \frac{\partial}{\partial x} & -C_2 \frac{\partial}{\partial y} \\ 0 & 0 & \frac{\partial}{\partial y} & 0 & 0 & C_1 & 0 \\ 0 & 0 & \frac{\partial}{\partial x} & 0 & 0 & 0 & C_1 \\ 0 & 0 & 0 & -3C_4 & 0 & -3C_2 & 0 \\ 0 & 0 & 0 & 0 & -3C_4 & 0 & -3C_2 \end{bmatrix} \quad (2.24)$$

The strain displacement matrix $[B]$ for the i^{th} node can be written as,

$$[B_i] = [\mathcal{L}]N_i \quad (2.25)$$

and $[K]^{(e)}$ the element stiffness matrix is,

$$[K]^{(e)} = \int_{A^{(e)}} [B]'[D][B]dA \quad (2.26)$$

Transforming from x, y co-ordinate system to natural co-ordinate system ξ, η , the stiffness matrix is represented as

$$[k]_{ij} = \int_{-1}^{+1} \int_{-1}^{+1} [B_i]'[D][B_j]det[j]d\xi d\eta \quad (2.27)$$

Here $[B_i]'$ is the transpose of matrix $[B_i]$ and,

$$[B_i] = \begin{bmatrix} N_{i,x} & 0 & 0 & 0 & 0 & 0 & 0 \\ 0 & N_{i,y} & 0 & 0 & 0 & 0 & 0 \\ N_{i,y} & N_{i,x} & 0 & 0 & 0 & 0 & 0 \\ 0 & 0 & 0 & 0 & 0 & 0 & C_1 N_{i,x} \\ 0 & 0 & 0 & 0 & 0 & C_1 N_{i,y} & 0 \\ 0 & 0 & 0 & 0 & 0 & C_1 N_{i,x} & C_1 N_{i,y} \\ 0 & 0 & 0 & 0 & -C_4 N_{i,x} & 0 & -C_2 N_{i,x} \\ 0 & 0 & 0 & -C_4 N_{i,y} & 0 & -C_2 N_{i,y} & 0 \\ 0 & 0 & 0 & -C_4 N_{i,x} & -C_4 N_{i,y} & -C_2 N_{i,x} & -C_2 N_{i,y} \\ 0 & 0 & N_{i,y} & 0 & 0 & C_1 & 0 \\ 0 & 0 & N_{i,x} & 0 & 0 & 0 & C_1 \\ 0 & 0 & 0 & -3C_4 N_i & 0 & -3C_2 N_i & 0 \\ 0 & 0 & 0 & 0 & -3C_4 N_i & 0 & -3C_2 N_i \end{bmatrix} \quad (2.28)$$

$$[J] = \begin{bmatrix} \frac{\partial x}{\partial \xi} & \frac{\partial y}{\partial \eta} \\ \frac{\partial x}{\partial \eta} & \frac{\partial y}{\partial \xi} \end{bmatrix}$$

$$= \begin{bmatrix} \frac{\partial \sum_{r=1}^{NN} N_r x_r}{\partial \xi} & \frac{\partial \sum_{r=1}^{NN} N_r y_r}{\partial \xi} \\ \frac{\partial \sum_{r=1}^{NN} N_r x_r}{\partial \eta} & \frac{\partial \sum_{r=1}^{NN} N_r y_r}{\partial \eta} \end{bmatrix} \quad (2.29)$$

When numerical integration is adopted, $[k]_{ij}$ becomes,

$$[k]_{ij} = \sum_{p=1}^N \sum_{q=1}^N W_p W_q [B_i]' [D] [B_j] \det[J] \quad (2.30)$$

W_p, W_q are weights used in Gaussian quadrature.

2.6 Strain energy of the laminate

The total strain energy is the sum of strain energy of individual elements

$$\begin{aligned} U &= \sum_{e=1}^{NE} U^{(e)} \\ &= \sum_{e=1}^{NE} \frac{1}{2} \int_{A^{(e)}} \{\bar{\epsilon}\}' [D] \{\bar{\epsilon}\} dA \end{aligned} \quad (2.31)$$

where NE is the number of finite elements into which the problem domain has been divided.

Substituting the above equation in equation.2.23, we get

$$U^{(e)} = \frac{1}{2} \int_{A^{(e)}} \left\{ \{\delta\}' [\mathcal{L}]' [D] [\mathcal{L}] \{\delta\} \right\} dA \quad (2.32)$$

Substituting for δ from equation 2.18 in equation 2.32, it may be put as

$$U^{(e)} = \frac{1}{2} \int_{A^{(e)}} \left\{ \left(\sum_{i=1}^{NN} \{\delta_i\}' [\mathcal{L}]' N_i \right) [D] \left(\sum_{i=1}^{NN} [\mathcal{L}] N_i \{\delta_i\} \right) \right\} dA \quad (2.33)$$

Further using Eqn.2.25 in Eqn.2.33 yields,

$$U^{(e)} = \frac{1}{2} \int_{A^{(e)}} \left(\{d\}' [B]' [D] [B] \{d\} \right) dA \quad (2.34)$$

2.7 Potential energy of the external load

A plate can be subjected to many types of loading such as the in-plane loading, moment loading, shear loading and out of plane loading. For the present analysis two types of out of plane loading is considered namely the sinusoidally varying and the uniform loading.

The potential developed due to the external lateral load is given by

$$V = \sum_{e=1}^{NE} V^{(e)} \quad (2.35)$$

Where, the element load vector is,

$$V^{(e)} = - \int_{A^{(e)}} \{\delta\}' \{\bar{q}\} dA \quad (2.36)$$

Here in this study only the transverse load is applied the loads corresponding to all other DOF is kept zero and thus the load vector is given by,

$$\{\bar{q}\} = \{0 \ 0 \ q(x, y) \ 0 \ 0 \ 0 \ 0\} \quad (2.37)$$

$q(x, y)$ is distributed load acting on the plane of the plate. For uniform loading

$$q(x, y) = q_0 \quad (2.38)$$

and for sinusoidally varying load.

$$q(x, y) = q_0 \sin \frac{\pi x}{a} \sin \frac{\pi y}{b} \quad (2.39)$$

Substituting for $q(x, y)$ in expression for V in Eqn.2.36, we get

$$\begin{aligned} V^{(e)} &= - \int_{A^{(e)}} \left(\sum_{i=1}^{NN} N_i \{\delta_i\}' \right) \{\bar{q}_i\}^{(e)} dA \\ &= - \{d\}^{(e)'} \{F\}^{(e)} \end{aligned} \quad (2.40)$$

where,

$$\{F\}^{(e)} = \int^{(e)} [N]^{(e)} \{\bar{q}\}^{(e)} dA \quad (2.41)$$

$F^{(e)}$ is the elemental load vector. It is obtained by assembling the nodal sub-vectors.

The elemental load vector in terms of sub-vector can be written as,

$$\{F\}^{(e)} = \sum_{i=1}^{NN} \{g_i\} \quad (2.42)$$

Where g_i , is given by

$$\{g_i\} = \sum_{p=1}^N \sum_{q=1}^N W_p W_q \det[J] N_i \{\bar{q}_i\} \quad (2.43)$$

Hence the load acting on i^{th} node of the element is obtained by

$$g_{i3} = \sum_{p=1}^N \sum_{q=1}^N W_p W_q \det[J] N_i q_{i3} \quad (2.44)$$

2.8 Total potential

For a conservative system, the total potential is stationary at the equilibrium configuration.

If U is the strain energy or the internal potential developed and V is the potential of the system due external workdone, the total potential of the system is given by

$$\delta(U + V) = 0$$

$$\delta \left(\prod_p \right) = 0 \quad (2.45)$$

Hence,

$$\prod_p = U + V = \text{Constant} \quad (2.46)$$

Further we can write,

$$\begin{aligned} \delta \left\{ \sum_{e=1}^{NE} \{d\}^{(e)'} [K]^e \{d\}^{(e)} - \{d\}^{(e)'} \{F\}^{(e)} \right\} &= 0 \\ \delta \left\{ \{d\}' [K] \{d\} + \{d\}' \{F\}^{(e)} \right\} &= 0 \end{aligned} \quad (2.47)$$

where $\{d\}$ is the global displacement vector, $[K]$ is the global stiffness matrix and $\{F\}$ is the global load vector. These are defined as

$$\begin{aligned} \{d\} &= \sum_{e=1}^{NE} \{d\}^{(e)} \\ &= \sum_{e=1}^{NE} [K]^{(e)} \\ \{F\} &= - \sum_{e=1}^{NE} \{F\}^{(e)} \end{aligned} \quad (2.48)$$

Equation.2.47 may be rewritten as,

$$\delta \{d\}' ([K] \{d\} + \{F\}) = 0 \quad (2.49)$$

The variational Eqn.2.49 leads to a set of linear equations of the form,

$$[K] \{d\} + \{F\} = 0 \quad (2.50)$$

The above Equation 2.50 is the governing equation of flexure for laminated composite plates. This equation is solved incorporating appropriate boundary conditions to obtain the displacement vector. The formulation presented herein was implemented in HP9000 series machine. The governing equation has been solved using system(NAG) library routines.

Chapter 3

Solution approach - Monte Carlo technique

The problem of analysis of composite structures with variation in material properties using Monte Carlo approach can be broken down into the following steps :

1. Random input sample generation.
2. System analysis.
3. Post processing of response behavior.

These steps are represented by a block diagram in Fig.3.1

3.1 Input sample generation

3.1.1 Number generator

A set of random numbers are generated of a given sample size, mean and standard deviation. These numbers are then manipulated in such a way that these have a Gaussian

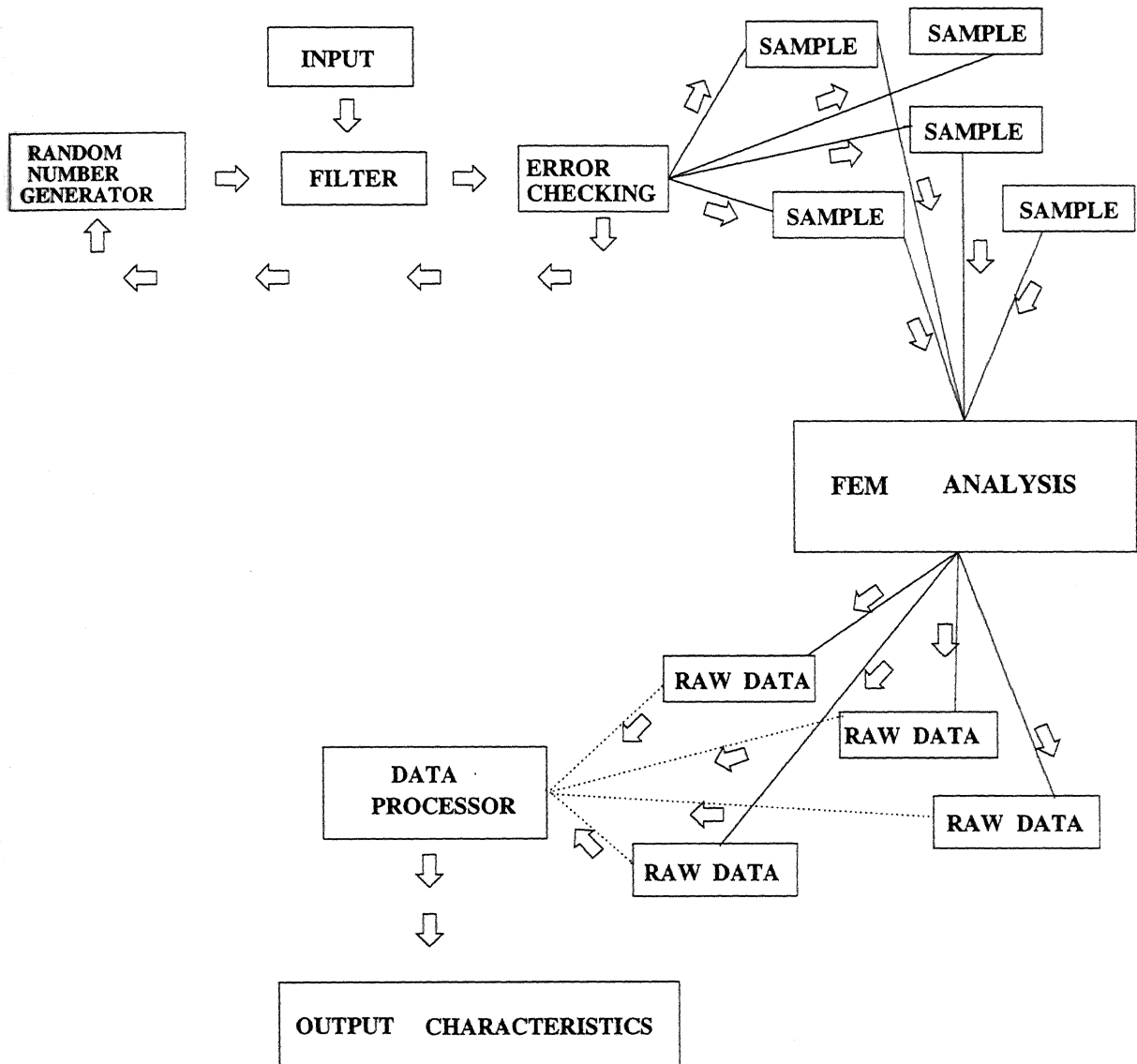


Figure 3.1: Lay-out of the code developed

3.1.2 Preprocessing of raw data

To get an input sample with desired characteristics, the pseudo random numbers generated by G05FDF are preprocessed before feeding them as input to the FEM analyser. The samples are checked for shift in the input mean(μ_{input}) and standard deviation(σ_{input}) which are usually present in a small amount, depending on the arithmetic of the computer employed.

1. Removal of shift in SD

The standard deviation σ of a raw data can be obtained from the relation for the variance σ^2 .

$$(\sum_{i=1}^n \frac{(x_i - \mu)^2}{n}) = \sigma^2 \text{ one can write } \epsilon_{SD} = \frac{\sigma_{desired}}{\sigma}$$

Each number is multiplied by the factor ϵ_{SD} to get a sealed sample with $\sigma_{desired}$ as the standard deviation.

2. Removal of shift in the mean

Let x_i ($i = 1, 2, \dots, n$) be a set of pseudo random numbers,

$$\text{then, } \sum_{i=1}^n x_i / n = \mu$$

where, μ is the mean of the generated numbers.

After the sample is checked for the error in standard deviation, the sample with $\mu_{desired}$ is obtained by offsetting each of the x_i by a constant ϵ , where $\epsilon_{mean} = \mu - \mu_{desired}$. The conditions for offsetting are :

if $\epsilon < 0$ the sample with $\mu_{desired}$ is obtained by adding ϵ to each number, in the case where $\epsilon > 0$ the numbers are reduced by ϵ .

The preprocessing is achieved by implementing the steps in succession. For this the statistical averaging subroutine (NAG-G01AAF) is combined with the random number generator (NAG-G05FDF). These samples are subsequently used as the input to the finite element analyser to study the plate deflection behavior.

3.2 System analysis

The governing equation of the bending of anisotropic laminated composites has been solved with the help of the finite element technique. A 7-DOF C^0 continuity model with 9-noded Lagrangian element is employed here. The presented analyser have been organized into following modules.

1. Mesh Generation Module.
2. Constituent Matrix and Force Vector Module.
3. The Solver.

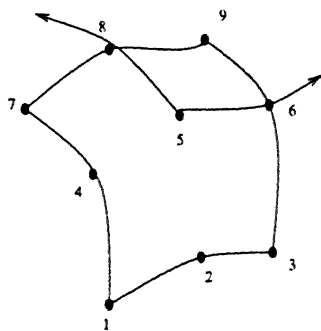
The plate is discretized into various elements. The mesh generation module generates the nodal co-ordinates for each element. Subsequent to this it generates the connectivity matrix and identifies the elements and their respective nodes on the boundary. With this mesh generation scheme full plate and quarter plate analysis can be performed. The boundary conditions are appropriately applied for both the cases. The code also can generate co-ordinates, connectivity and apply boundary conditions for plate with any shape of cut-out. The module generates a uniform mesh around the cut-out with quadrilateral elements. The mesh for the plate with cut-out is generated only for quarter plate. The routine has the capacity to generate mesh for arbitrarily shaped cut-outs, provided the shape is represented as polar function $f(r, \theta)$. As the thickness (h), individual ply-orientation and the material properties are given, a general constituent matrix is developed. With simple changes in the input data isotropic, orthotropic and anisotropic constituent matrices can be developed. This along with the element co-ordinates go to form the element stiffness matrices. Element stiffnesses are assembled with the help of connectivity matrix and boundary conditions are appropriately applied to the boundary elements. With the information about the nature of loading the element force vector is generated and assem-

bled. The assembled global stiffness matrix and the global force vector constitute a set of linear equations. NAG F04ATF solver is used to get the respective deflections depending on the type of the plate analyzed. The deflections obtained from the developed FE model has been validated against results of standard HSDT models [13, 14].

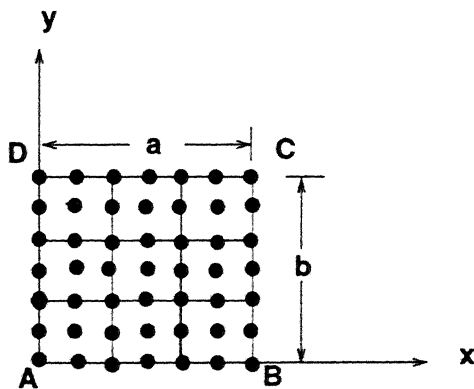
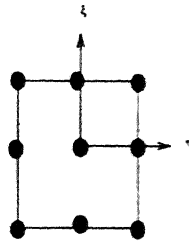
3.3 Post processing of the response behavior

The sample of the deflection response of the plate is obtained from the system FEM analyser. Its statistical information is extracted by feeding the obtained data sample to the routine G01AAF. This routine gives the mean and the standard deviation of the fed data.

The above scheme is used for obtaining the displacement characteristics with the basic material properties varying individually as well as simultaneously for plates with and without cut-outs. These are presented graphically in Chapter 4.



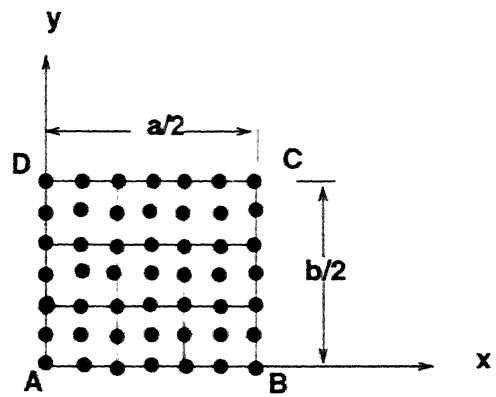
Nine-noded biquadratic Lagrangian element



Full Plate

Boundary conditions

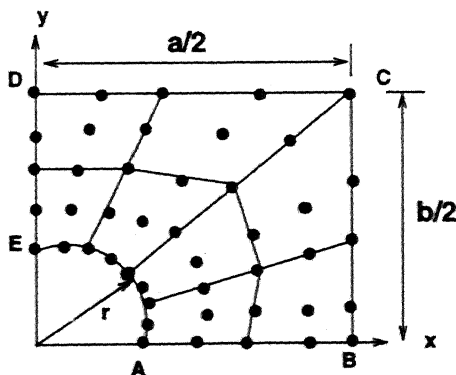
For SS	Along AB, CD	$U=W=\theta_x=\psi_x=0$
	Along BC, AD	$V=W=\theta_y=\psi_y=0$
For CC	Along AB, CD	$U=V=W=\theta_x=\theta_y=\psi_x=\psi_y=0$
	Along BC, AD	$U=V=W=\theta_x=\theta_y=\psi_x=\psi_y=0$



Quarter Plate

Boundary conditions SS

Along AB	$v=\psi=\theta_x=0$	Symmetry Line
Along AD	$u=\theta_x=\psi_x=0$	Symmetry Line
Along BC	$v=w=\theta_y=\psi_y=0$	
Along CD	$u=w=\theta_x=\psi_x=0$	



Mesh for plate with cut-out

Boundary conditions

Along AB	$v=\psi=\theta_x=0$
Along BC	$v=w=\theta_y=\psi_y=0$
Along CD	$u=w=\theta_x=\psi_x=0$
Along DE	$u=\theta_x=\psi_x=0$

Convergence Study

Mesh Size	$\bar{w} \times 10^{-2}$
2x2	4.397522
3x3	4.616823
4x4	4.645705
5x5	4.643798

A Plate Without Cut-out

$$a/b=1.0$$

$$a/h=10.0$$

Isotropic plate SS

$$\bar{W} = w \cdot E t h^{3/4} / q \cdot a^{3/4}$$

$$Nu=0.3$$

$$q=100 \text{ N/m}^2$$

Mesh Size	$w \times 10^{-7} \text{ m}$
2x2	4.2506
3x3	4.3376
4x4	4.0296
5x5	4.1436
6x6	4.0031

B Plate With Cut-out

$$a/h=4$$

$$a/b=1.0$$

$$l/d=10.0$$

$$[45/-45/45/-45]$$

$$q=1000 \text{ N}$$

SS

$$a=1\text{m}$$

Validation Study for Composites

$$q=100 \quad a/b=1.0$$

Type	a/h	θ	\bar{W}	FSDT _[15]	HSDT _[15]
Uniform	10	15	0.9459	0.9698	0.9512
		30	0.9157	0.9518	0.9302
		45	0.8790	0.8919	0.8708
	100	15	0.6962	0.7095	0.7090
		30	0.7537	0.7690	0.7686
		45	0.7428	0.7284	0.7281
Sinusoidal	10	15	0.5970	0.6350	0.6218
		30	0.5748	0.6167	0.6015
		45	0.5501	0.5765	0.5618
	100	15	0.4374	0.2765	0.2763
		30	0.4680	0.4555	0.4551
		45	0.4585	0.4694	0.4592

$$\bar{W} = [E t h^{3/4} / (q a^{3/4})] w \quad E l = 40.0 E t, G l t = G t p = 0.6 E t, G t p = 0.5 E t, N u l t = 0.25$$

Chapter 4

Results and Discussion

The approach presented in the previous chapter is used to obtain the deflection statistics of rectangular plates. This chapter is organized in two sections. In the first section the behavior of rectangular plate with different support conditions has been studied for change in material property variation over a range and in the next section the study is conducted for rectangular plates with cut-outs. Initially the effect of randomness in individual material property has been studied to identify the most critical parameter. In the latter section a problem of practical importance is dealt with assuming all the material properties to vary randomly and simultaneously.

- Samples are generated with the standard deviation varying from 2 percent to a of 20 percent of their mean values with sample-size 1000 and 10 such samples are used for each study.
- The material properties considered to be random are $E_l, E_t, \nu_{lt}, G_{lt}$ and G_{tz} .

Results have been obtained for T300/52208 graphite/epoxy composite [6] with mean values as given below :

$$\begin{array}{ll}
E_l = 145.0 \text{ GPa} & G_{lt} = 4.5 \text{ GPa} \\
E_t = 10.71 \text{ GPa} & G_{tz} = 4.5 \text{ GPa} \\
\nu_{lt} = 0.31 & G_{tz} = 3.5906 \text{ GPa}
\end{array}$$

4.1 Deflection characteristics of rectangular plates

In this section we study the effect of dispersion in individual input random variables while the characteristics of the other input variables are kept constant on plates with different aspect-ratios(AR), boundary conditions, ply-orientations and thickness-ratios(a/h). Here the variations are considered on a SS square antisymmetric laminate with ply-orientation $[45^\circ/-45^\circ/45^\circ/-45^\circ]$ and a/h of 10. In a given study except for the parameter selected all the other parameters are kept constant. The ARs chosen for the study are 2, 3 and 4. Two classical boundary conditions have been considered namely all edges SS and all edges CC. Results are obtained for 4-layered antisymmetric laminates with ply-orientation 15° , 30° and 45° and 0° . Three a/h s of 4(thick), 8 and 100(thin), are considered for the plate. The curves for $a/h = 100$ are multiplied by 10^{-3} in the case of E_l , E_t and ν_{lt} characteristics, and for the characteristics of G_{lt} and G_{tz} the factor is 10^{-1} .

Plate is uniformly loaded with $q = 1000 \text{ Nm}^{-2}$ and displacement refers to central displacement of the plate.

The Fig. 4.1 through Fig. 4.5 shows the response of the plate to each input RV. Each figure represents four different studies A, B, C and D. where A, B, C and D presents the effect of the SD of input RV on the SD of the central deflection of the plates with different boundary conditions, ARs, a/h s and ply -orientations.

Effect of Longitudinal Elastic Modulus E_l

Fig.4.1 gives the characteristics of the plate response with different standard deviation of E_l . The response shows a linear behavior for small σ_{E_l} . However, with increase in deviation the response becomes somewhat non-linear. The non-linearity is stronger for some ply-orientations compared to the effects of support conditions, ARs and a/h . The dispersion in the displacement characteristics of the plate is found to be maximum for $a/h = 100$ (thin plate). The plate shows least sensitiveness to input dispersion for the $AR = 4$. There is a marked increase in sensitiveness of the plate response for $AR=2$ compared to the $AR=3$ and 4. The plate with all edges CC is more affected by change in input randomness compared to a plate with all edges SS. From the study of the effect of a/h it is found that variation in the characteristics is most prominent for thin, and least for thick plates. The 0° symmetric laminate is affected more and a 45° anti-symmetric laminate gets affected the least due to change in σ_{E_l} . However, the overall difference between the two is small indicating low sensitivity to ply-orientation.

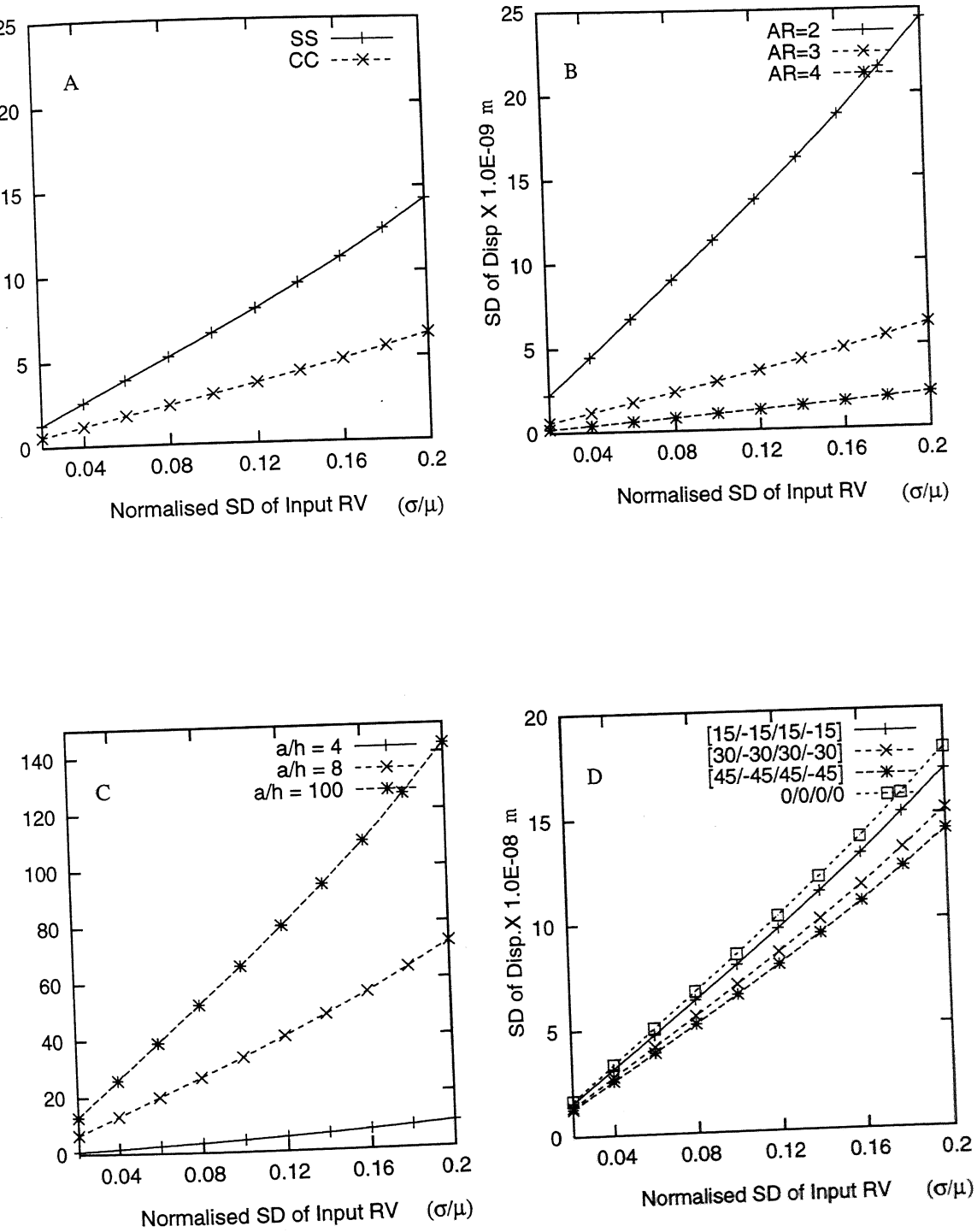


Figure 4.1: Plate deflection characteristic with σ_{E_l}

Effect of transverse elastic modulus E_t

The characteristics of the system with E_t as input random variable is presented in Fig.4.2. The general behavior is almost linear except for the plates with different ply-orientation, but unlike the case of E_l , here its slope shows a decreasing trend. The plate with AR=4 is least affected by change in the input randomness while the plate with $a/h = 100$ shows maximum effect. As observed in the case of E_l there is again a marked higher sensitiveness for plates with AR=2 as compared to plates with AR=3 and 4. All edges simply-supported plate is more affected by dispersion in E_t than all edges CC plate. The effect of the a/h is similar to that observed for E_l . The plate with 15° orientation is affected maximum and indicates higher sensitivity compared to the 0° symmetric case. The slope of the response characteristics are lower for the other two angles, reducing from 30° to 45° anti-symmetric case.

Effect of major Poisson's ratio ν_{lt}

The sensitivity of mid point displacement characteristics of the plate for variation in $\sigma_{\nu_{lt}}$ is given in Fig.4.3. The general nature of the curves are mostly linear. The least affected are the plates with $a/h = 4$ and plate with AR=4. On the other side the plates with ply-orientation 0° and $a/h = 100$ get affected the most. The effect of change in the AR shows a similar trend as discussed before for E_l and E_t . There is a reversal of trend for the two support conditions compared to the effect of E_l and E_t as the displacement characteristics of SS case is affected more than that of the CC edge one. As the ply orientation angle increases the response slope reduces, the reduction being stronger for small angles, indicating decreasing trend with increase in the ply angle.

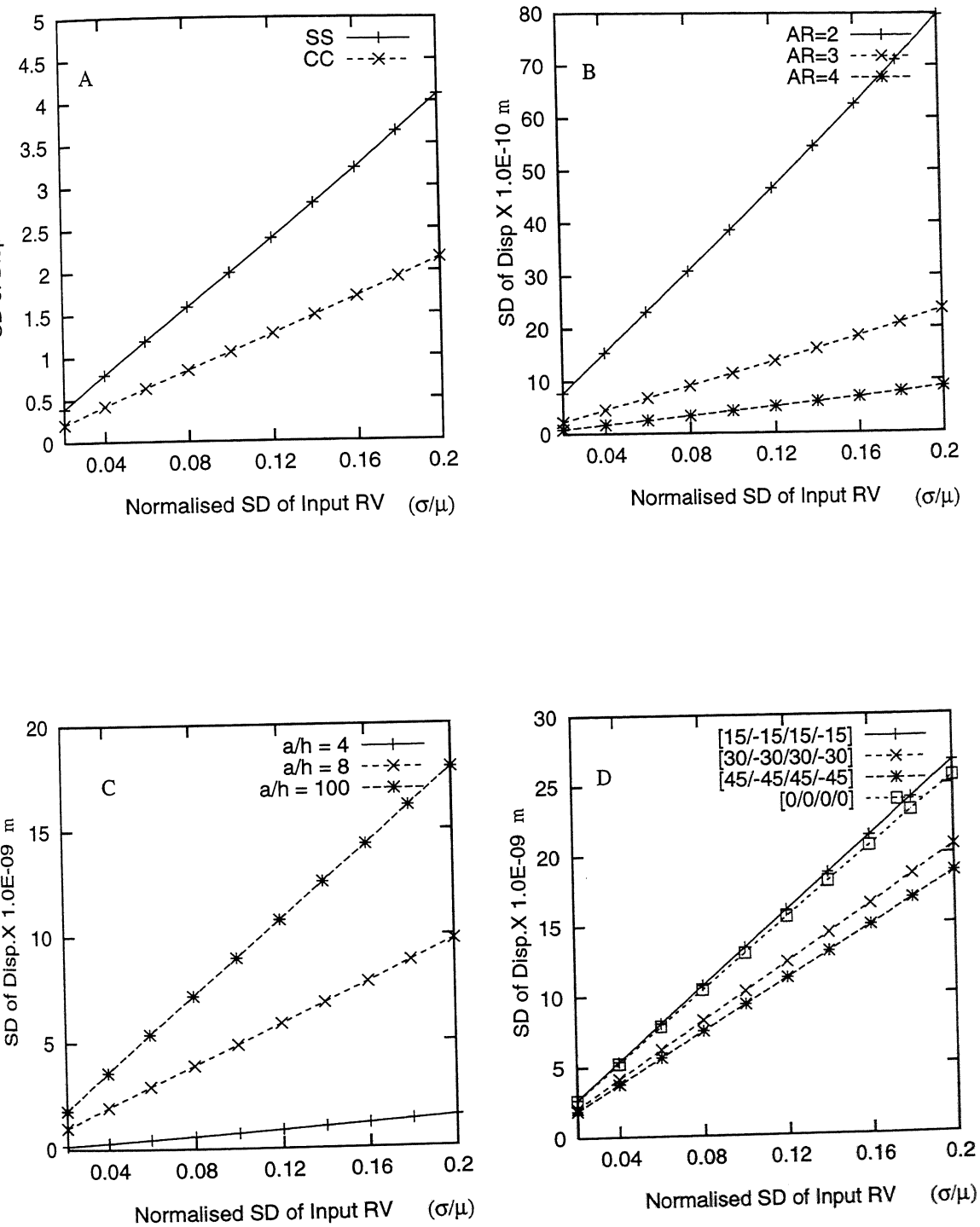


Figure 4.2: Plate deflection characteristic with σ_{Et}

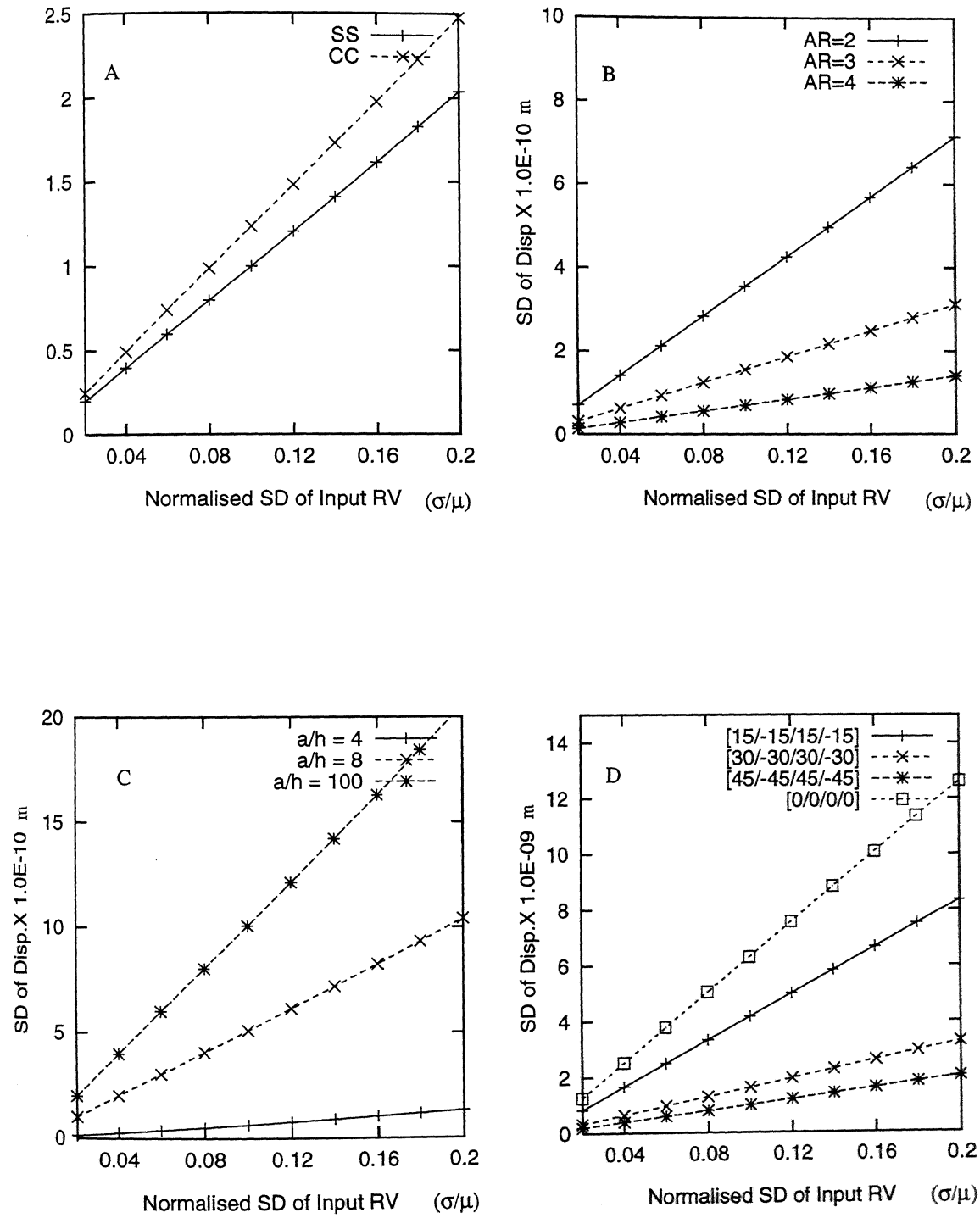


Figure 4.3: Plate deflection characteristic with $\sigma_{\nu_{lt}}$

Effect of rigidity moduli G_{lt} and G_{tz}

Fig. 4.4 shows the behavior the system for input random variables G_{lt} and G_{tz} . The characteristics are mostly linear. The 0° symmetric laminate and plate with $a/h = 100$ is affected maximum and the plate with $AR=4$ is affected the least for change in dispersion in G_{lt} and G_{tz} . The trend of all the characteristics, in general are similar to that of the ν_{lt} case. The response for a/h of 4 and 8 are close and much less compared to the case of $a/h = 100$.

Effect of rigidity modulus G_{lz}

The system behavior for input random variable G_{lz} is given by Fig. 4.5. Here too the characteristics are mostly linear and plate with $a/h = 100$ is affected the most and plate with AR of 4 is least affected. The response curves for both the boundary conditions almost coincide with each other, showing that behavior is not affected with the two boundary conditions considered. The behavior of all the other characteristics, in general resemble the G_{lt} case.

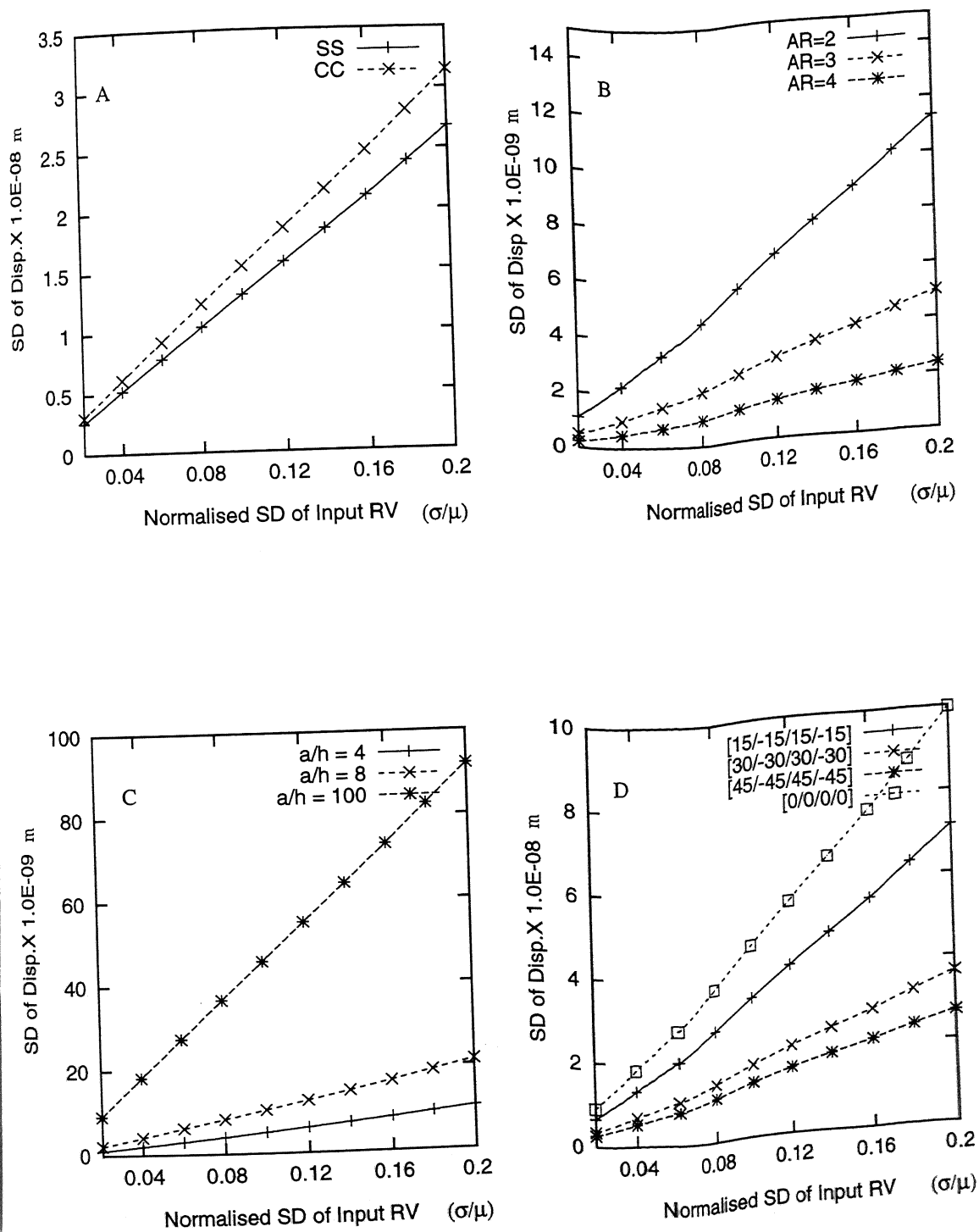


Figure 4.4: Plate deflection characteristic with $\sigma_{G_{tt}}$ and $\sigma_{G_{tz}}$

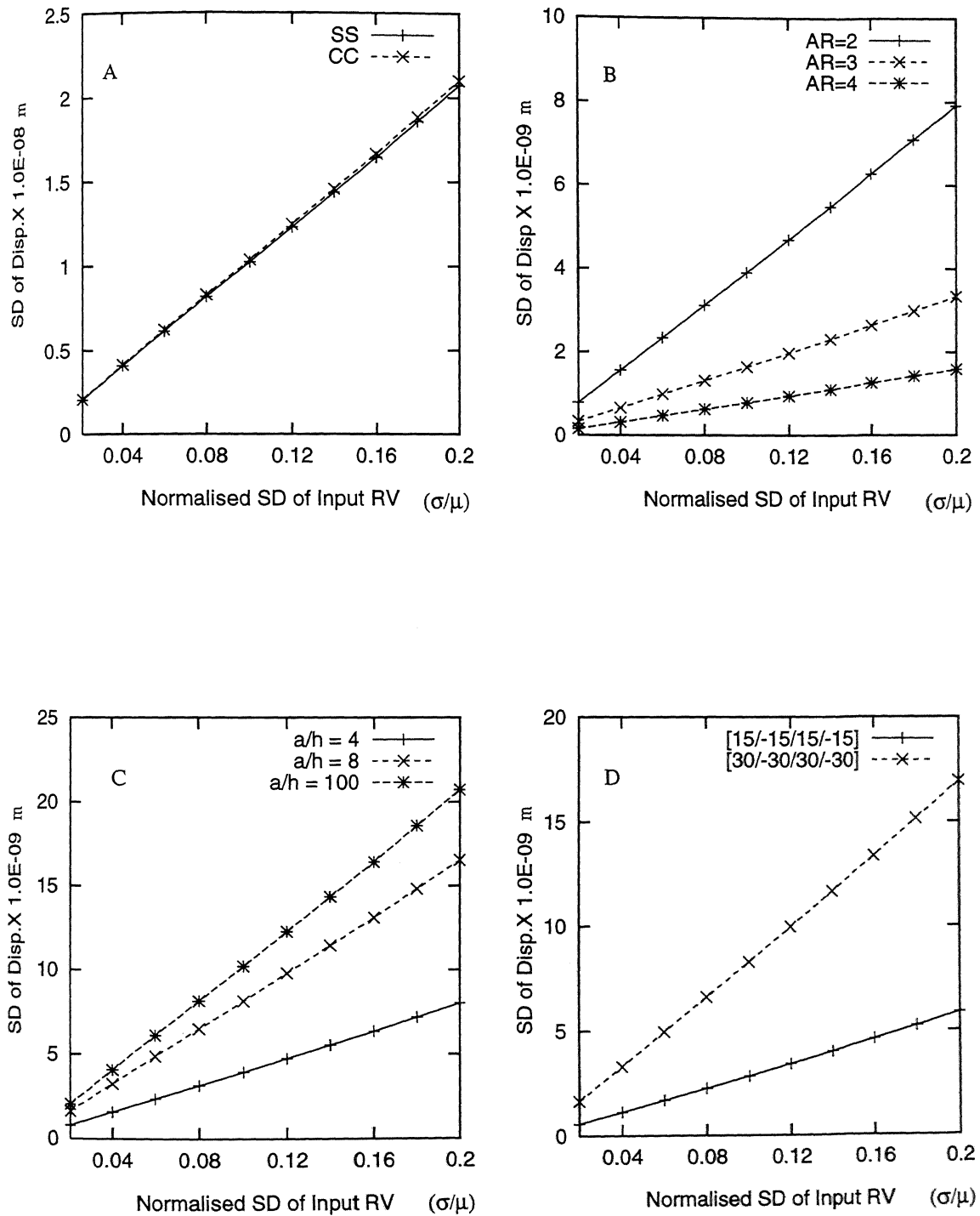


Figure 4.5: Plate deflection characteristic with σ_{G1z}

4.1.1 Response sensitivity

In this section, a comparative study between different plate configurations is carried out to highlight the quantitative sensitivity of the system to randomness in individual material properties. The transverse loading is assumed as uniformly distributed $1000Nm^{-2}$ and unless specified the ply-orientation is $[45^0 / -45^0 / 45^0 / -45^0]$. Four plates are used for the sensitivity study :

1. A square plate, with a/h of 10, CC at all edges.
2. A rectangular plate with $AR=2$ and $a/h=10$, with SS edges.
3. Square and moderately thick plate $a/h=8$, with SS edge conditions.
4. A square plate, with SS edges, $a/h = 10$ and ply-orientation $[15^0 / -15^0 / 15^0 / -15^0]$ and $a/h = 10$.

Fig.4.6 shows the deflection characteristics for the four plates for variations in the standard deviation of the material properties E_l , E_t , ν_{lt} , G_{lt} and G_{tz} . The material properties are taken to vary only one at a time, other being held constant at their mean values. It is seen that for the cases studied here the plate is most sensitive to the randomness in the longitudinal elastic modulus(E_l), the next most sensitive parameter being the rigidity modulus G_{lt} and G_{tz} , The remaining material parameters do affect the displacement characteristics but the effect is less than half the effect of the longitudinal modulus.

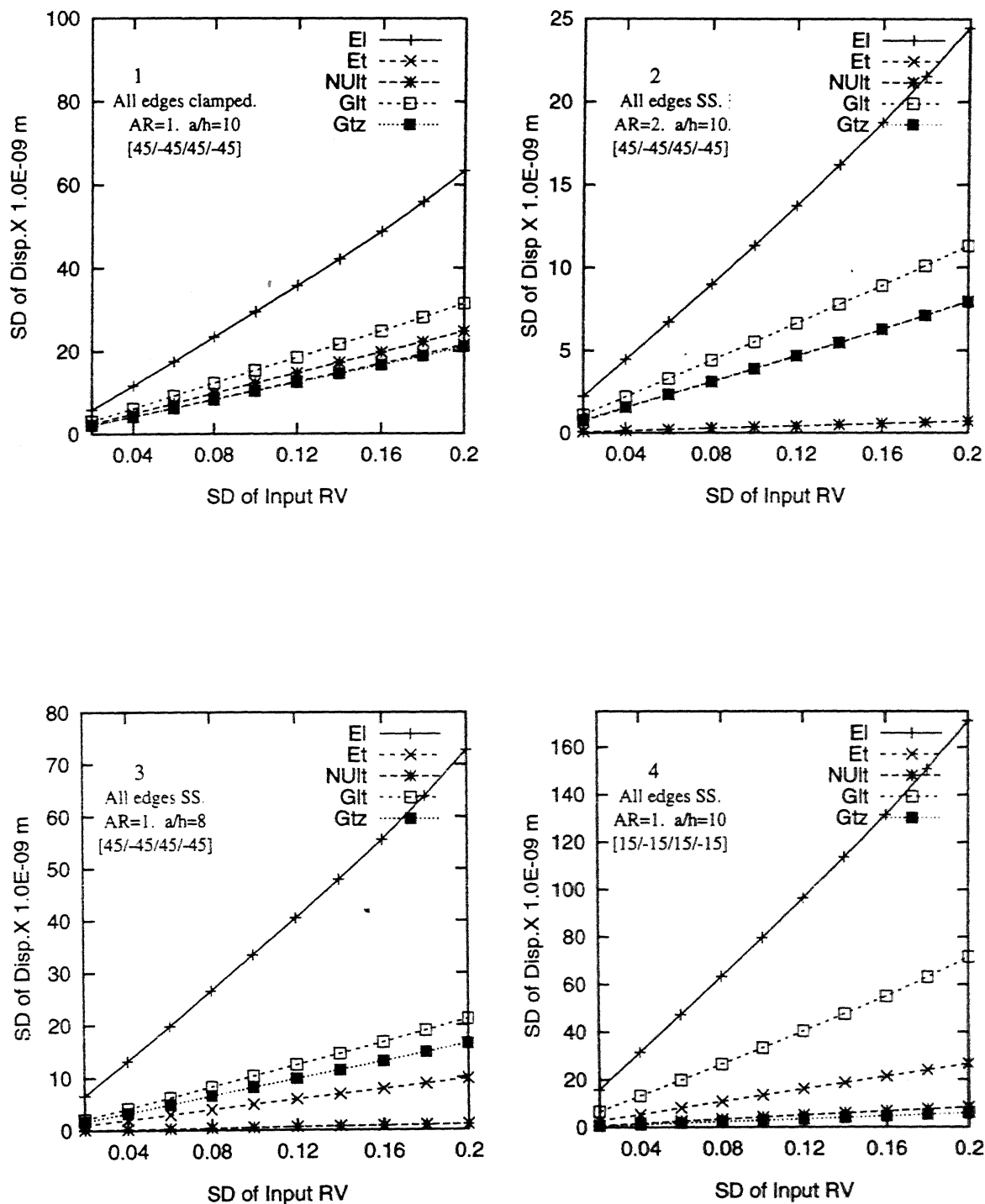


Figure 4.6: Response sensitivity of the composite plate to material properties

4.1.2 Normalised characteristics of composite plate

Effect of variation in standard deviation of the individual material properties, keeping the rest all constant, has been presented in detail in the preceding sections. From the applications point of view it is appropriate to consider the case where all the properties vary simultaneously. Fig.4.7 presents the normalised characteristics of the plate, with all the material properties varying simultaneously each assuming same value for the ratio of its standard deviation to mean.

The displacement standard deviation is normalised with the mean displacement of the plate obtained with all the material properties having their mean values. Fig. 4.7 shows the normalised behavior of the plate. It is observed that the proposed normalisation scheme when used, the different characteristic curves for different ARs happen to fall on each other, this is also true for the characteristic curves for a/hs and boundary conditions. The plate with $[45^\circ / -45^\circ / 45^\circ / -45^\circ]$ ply-orientation is least affected by the input randomness, and the 0° symmetric laminate has higher response slope. However, the dispersion in response characteristics for different ply-orientations is small. Fig. 4.8 is constructed by superimposing all the normalised curves. One can observe that the curves form a band which is non-linear in nature. The non-linearity enter into the characteristics beyond 10 percent of the input σ . The maximum dispersion in the characteristics is 1 percent and the curves lie in between a maximum σ_{output} of 23 to 24 percent for the normalised σ_{input} of 20 percent.

The interesting finding has raised queries whether the normalised characteristics of all plates behave in a similar way. Hence, further studies are pursued in this direction for plates with cut-outs and a different loading pattern.

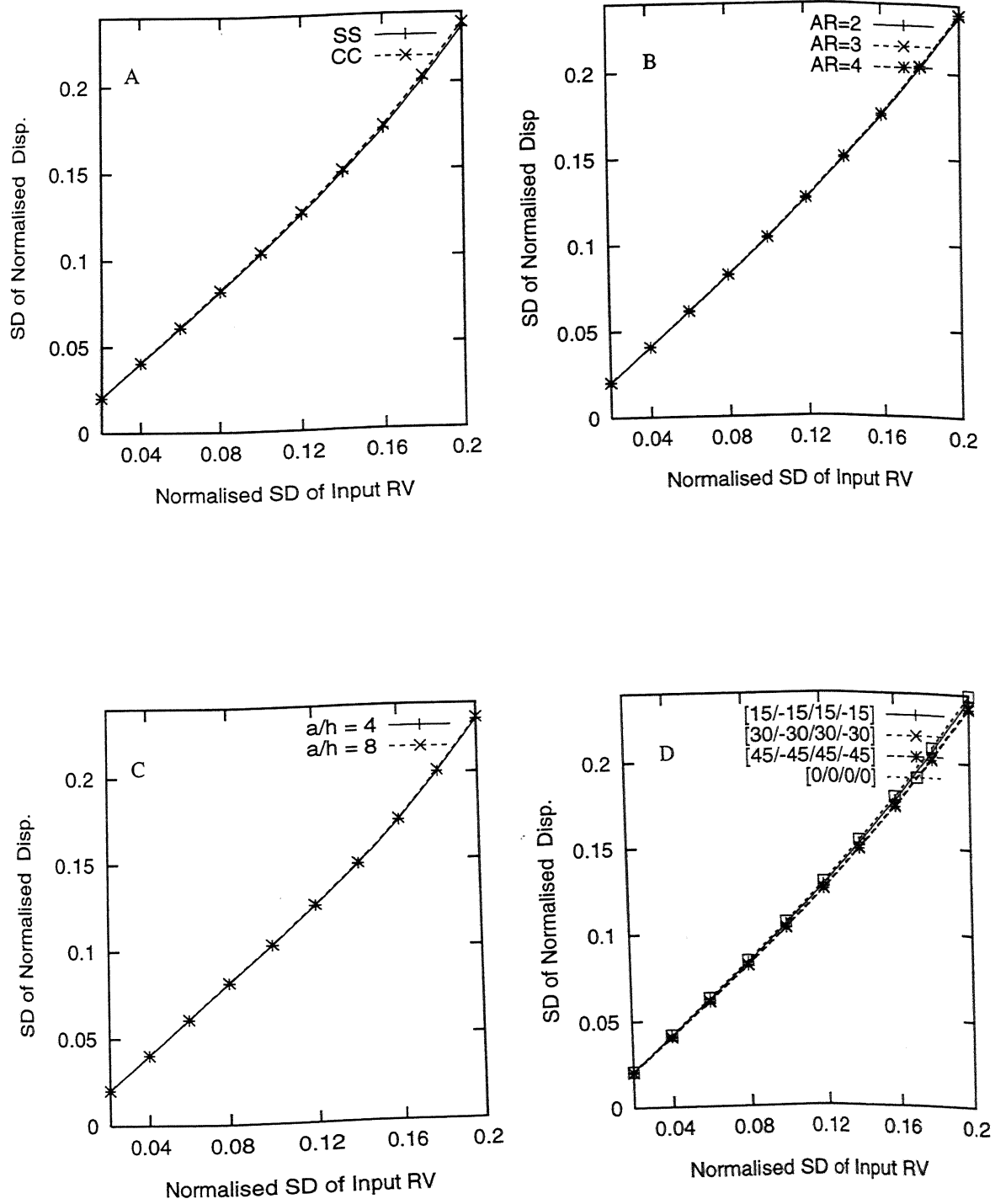


Figure 4.7: Normalised response characteristics of rectangular plates

Influence of randomness in all material properties

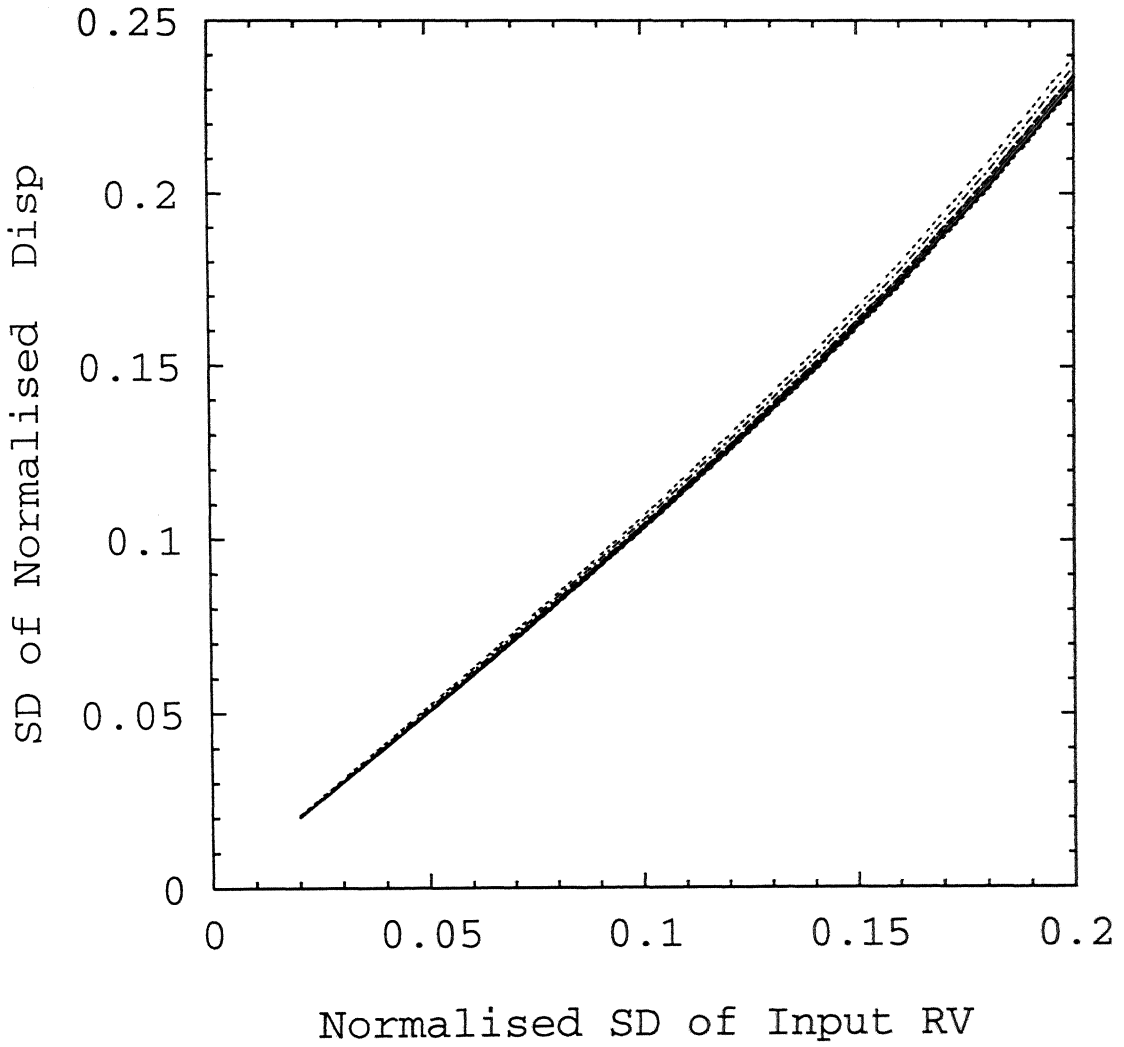


Figure 4.8: Superimposed plate response characteristics

4.2 Deflection of plates with cut-outs

In Aerospace structure applications weight reduction is an important applications design criteria. Besides being used due to functional requirements, cut-outs also have relevance to the problem of weight reduction. More and more structures are used with cut-outs. This motivated the study of the behavior of composite plates with cut-outs. The analysis approach developed can handle different shapes of cut-outs. Here, for the present study, circular cut-outs have been used in rectangular plates with plate length to cut-out diameter ratios or cut-out ratios (l/d) having values 2,4,6,8 and 10. A standard plate is taken with $AR = 1$, $a/h = 10$, ply-orientation $[45^\circ / -45^\circ / 45^\circ / -45^\circ]$. A sinusoidally varying distributed load of amplitude $1000N$ is used for this analysis. The displacement of the point located at the intersection of rim of the cut-out and the major axis of symmetry is monitored and taken for the study.

The normalisation scheme of the previous section is used here for the study. Plots are developed to bring out the effects of boundary conditions, ARs, a/h and ply-orientation for the five l/d ratios mentioned. Figs. 4.9.to 4.13 present normalised displacement characteristics of the plates with different l/d ratios. The use of this scheme brings forward anticipated interesting results. In these figures, it is observed that irrespective of the different configurations of the plate, such as different AR , boundary conditions, a/h and ply-orientations, their normalised displacement characteristic curves are very close, almost coincide with each other.

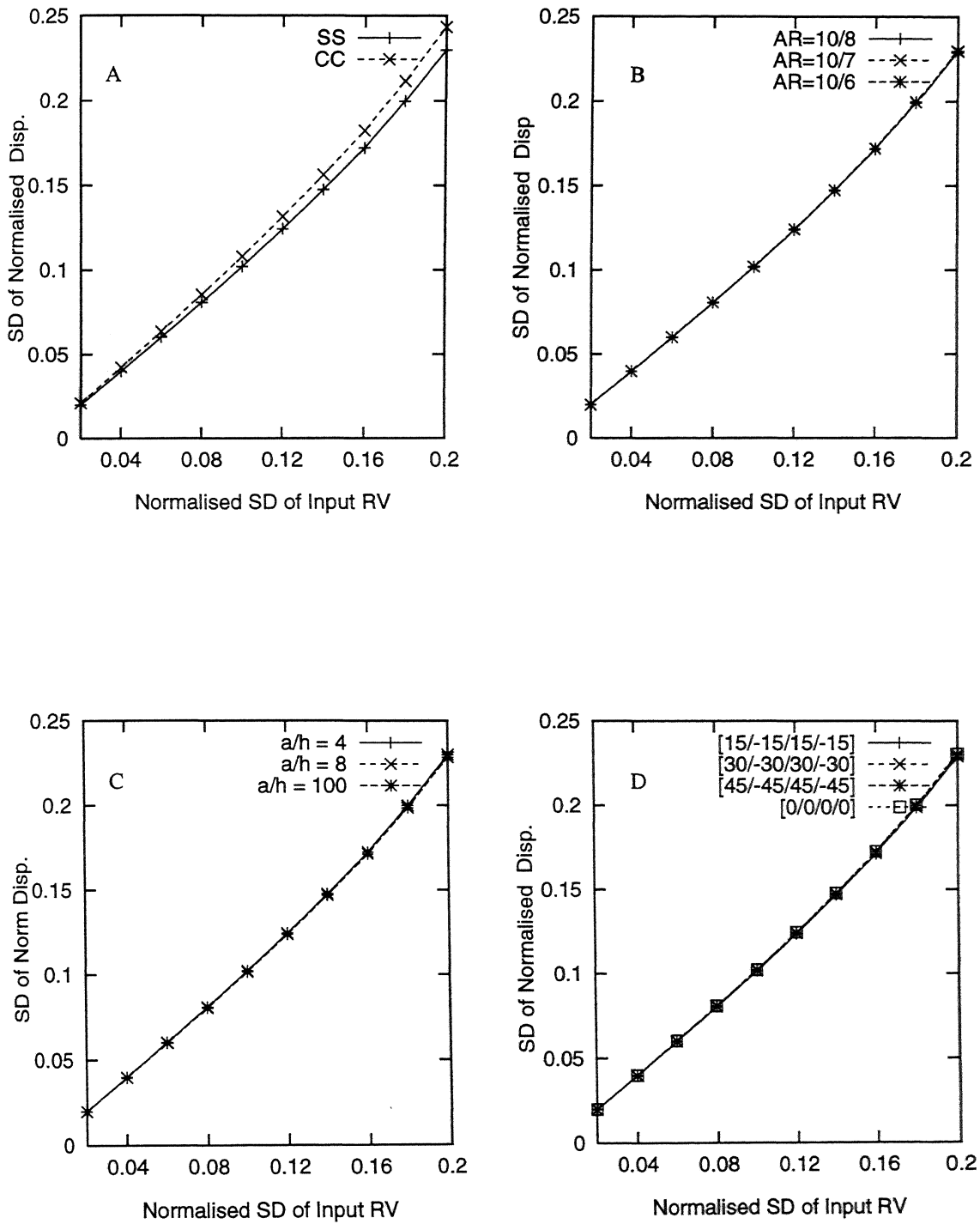


Figure 4.9: Characteristics of the composite plate with cut-out, $l/d = 2$

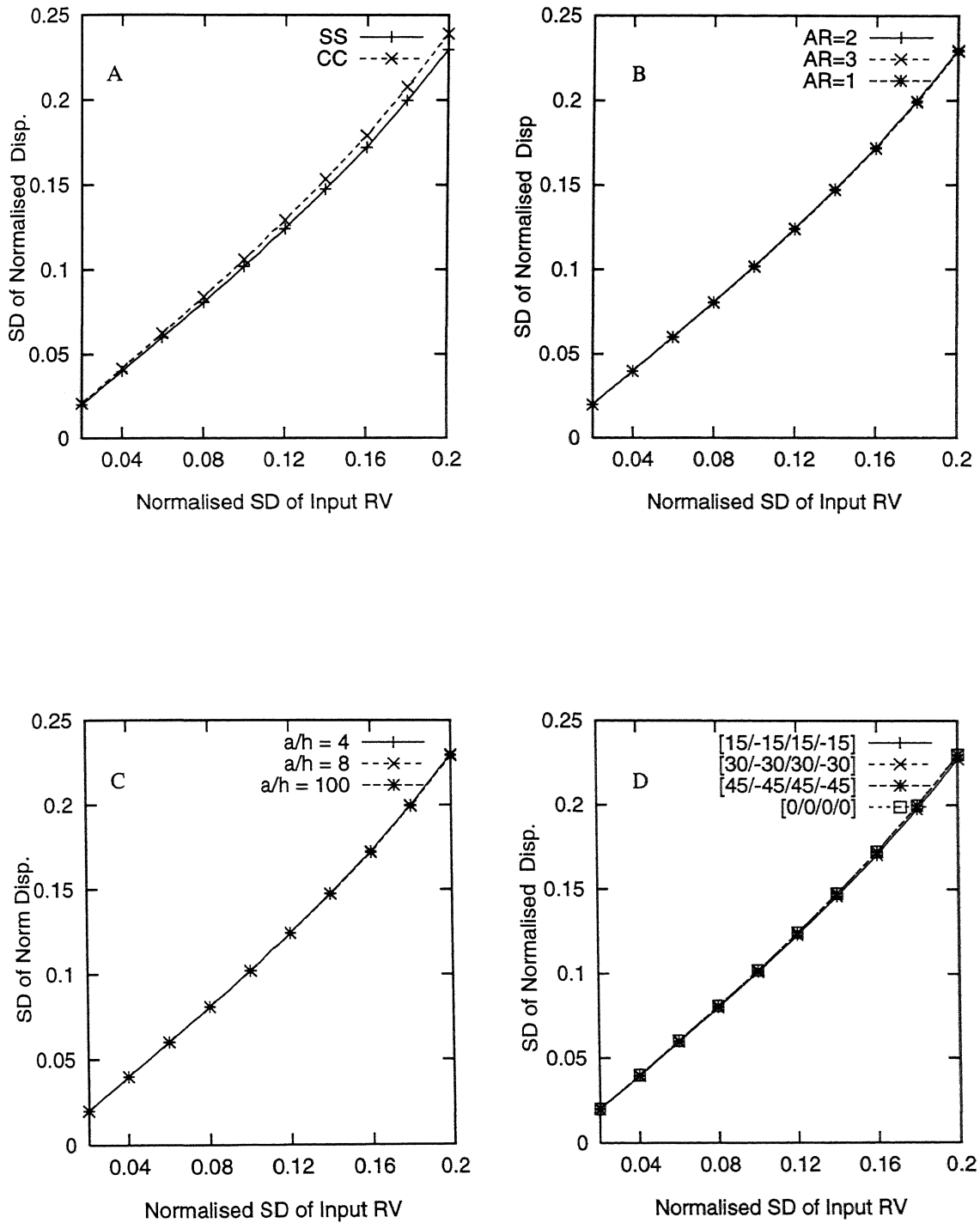


Figure 4.10: Characteristics of the composite plate with cut-out, $l/d = 4$

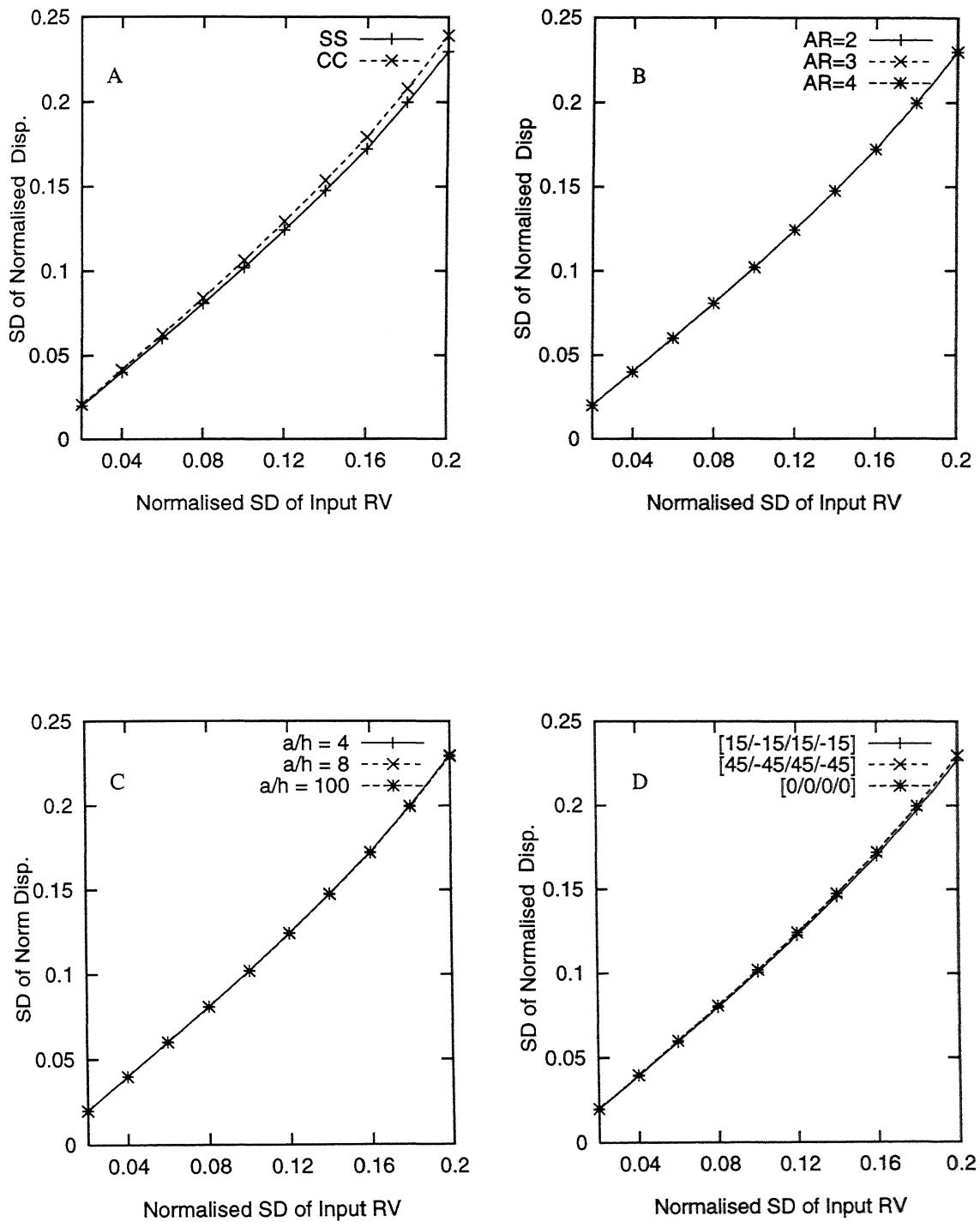


Figure 4.11: Characteristics of the composite plate with cut-out, $l/d = 6$

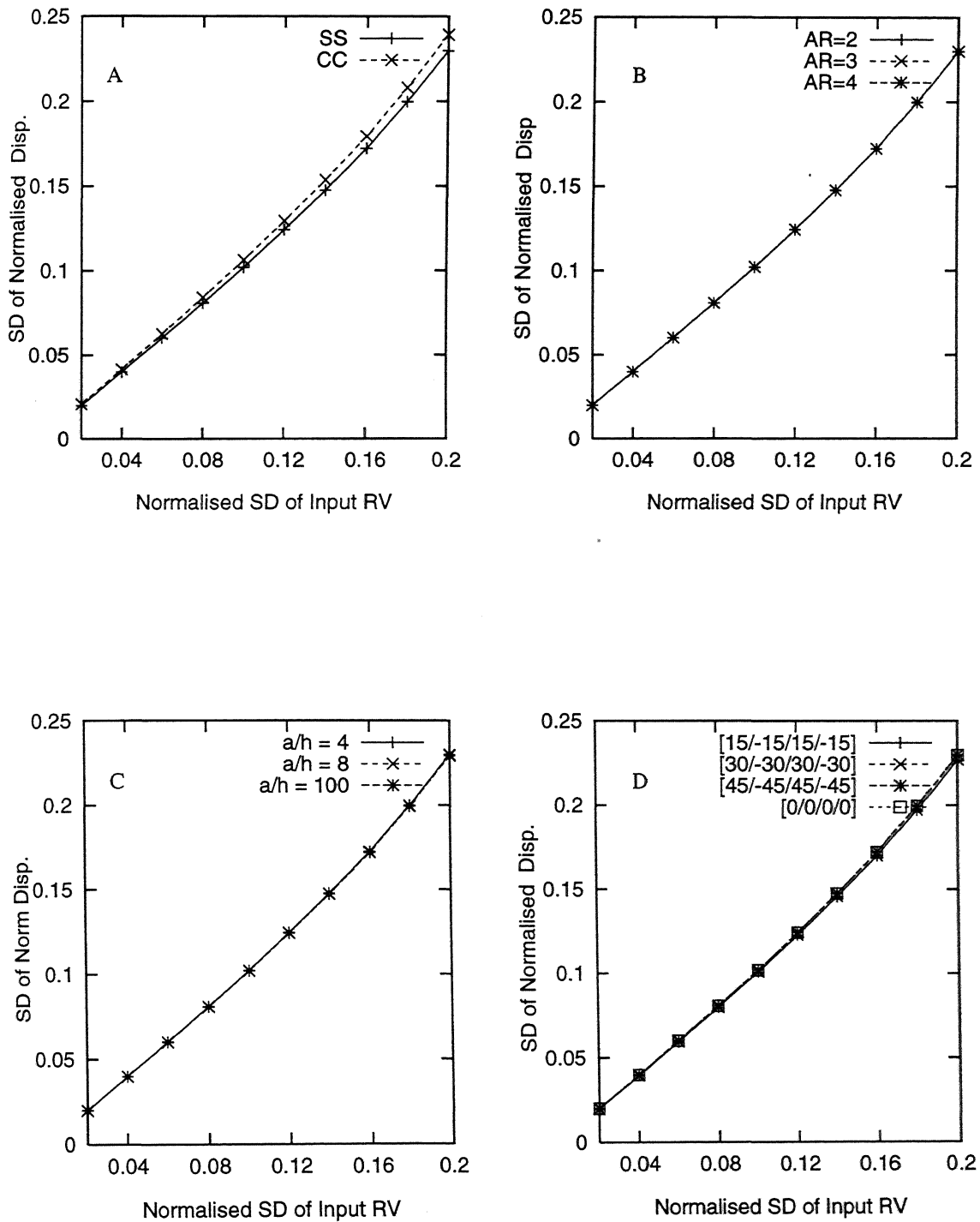


Figure 4.12: Characteristics of the composite plate with cut-out, $l/d = 8$

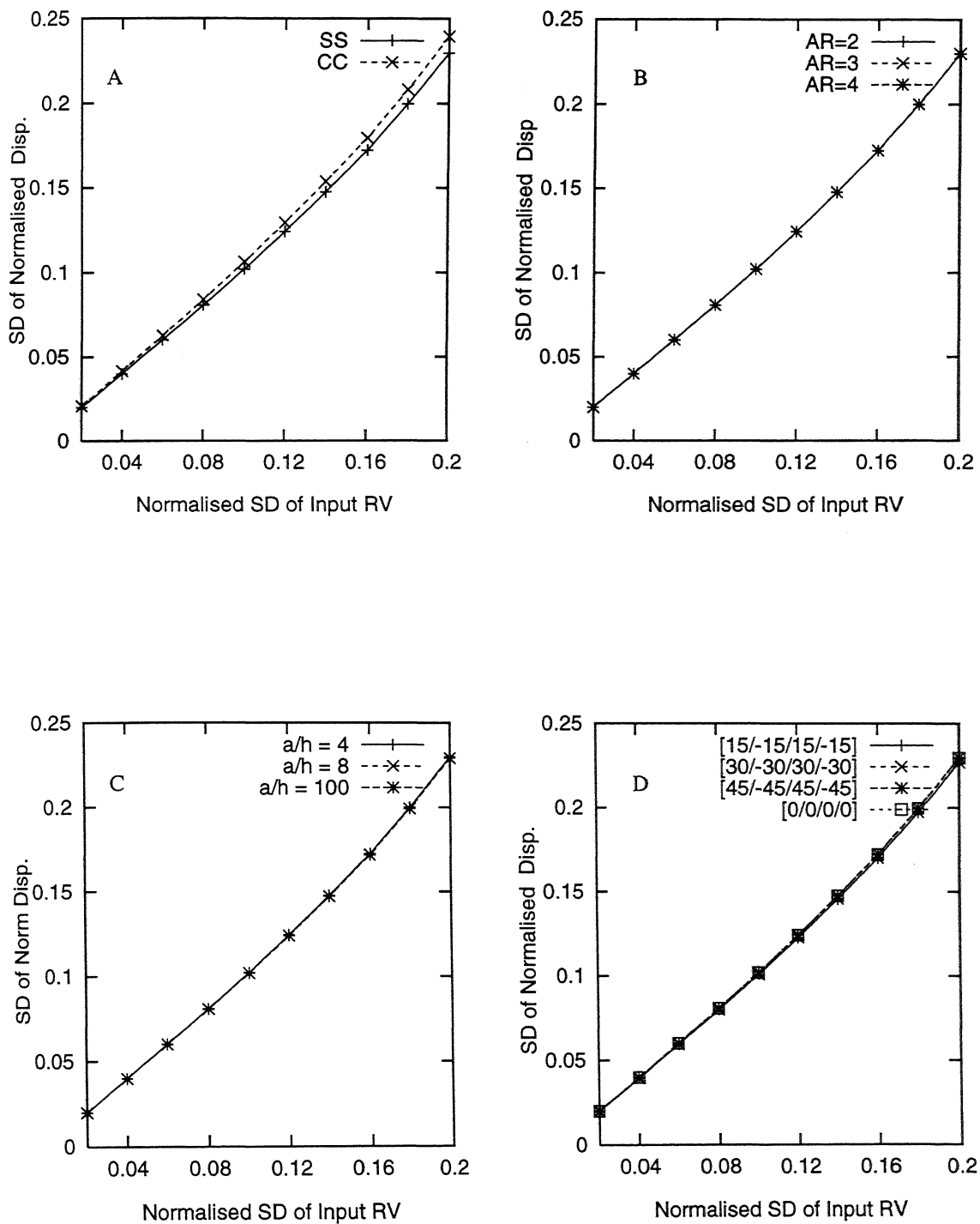


Figure 4.13: Characteristics of the composite plate with cut-out, $l/d = 10$

This aspect is further illustrated by the Fig. 4.14 , obtained by superposing all the Fig.4.9 through Fig.4.13. A marker line $y = x$ is included to show the deviation of these curves from linearity. The characteristic curves group themselves into two bands. The thicker band representing the behavior of these plates with SS edge condition and the band with maximum deviation is the characteristics of the plates with cut-out l/d ratios ranging from 2 to 10 and all edges CC. It is observed that normalised response characteristics is affected by different boundary conditions and the nature of the curves are linear up to 10 percent of the variation in the input characteristics, beyond this the the curves show a distinct non-linearity the deviations being, 23 percent for the SS plate and 24 percent for the CC plate for the input SD of 20 percent.

It can be inferred from these figures that the effect of variation in the randomness in the material property on different plates with different AR , a/h , support condition and fiber orientation may be presented in the normalised form in one similar way. In other words, the curve may be thought as a design curve which can predict the normalised characteristics for all the configurations mentioned. It is understood that from the normalised characteristics we can always obtain the absolute characteristics of any plate configuration.

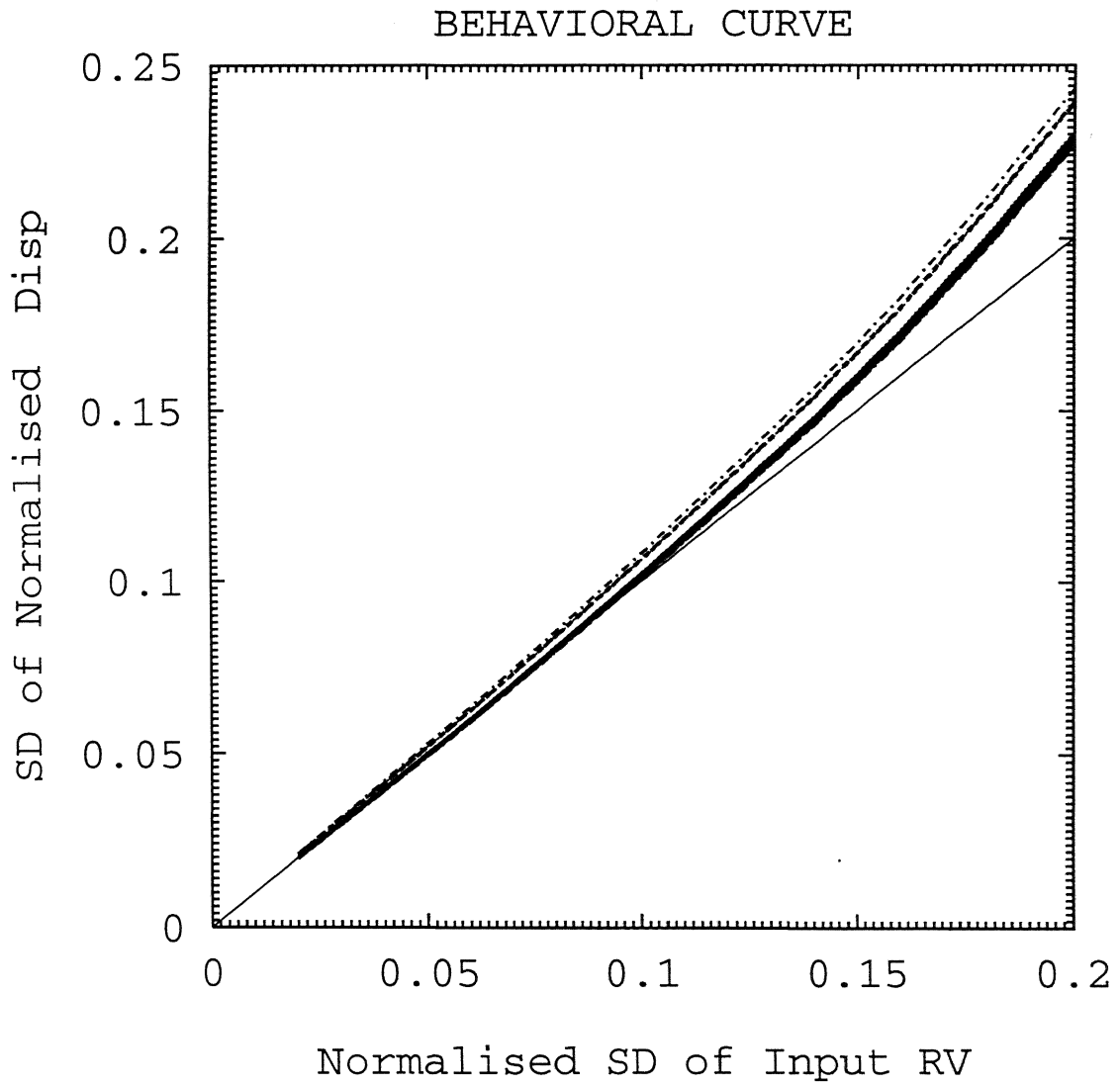


Figure 4.14: Characteristics of the plate with cut-out, $l/d=2$ to 10

Chapter 5

Conclusions and scope for future work

In this thesis, a statistical study of the bending behavior of composite laminated rectangular plates with different configurations has been carried out using finite element method. From this study the following main conclusions can be drawn.

1. The longitudinal modulus E_l and the rigidity modulus G_{lt} are the most critical of the material properties. They considerably influence the deflection characteristics of the composite plate.
2. The thin plate ($a/h = 100$) is most sensitive and the plate with AR=4 is least sensitive to the variation in input material property characteristics.
3. The behavior of the plate is found to be linear for low dispersion in material properties. For larger dispersion, with $(\frac{\sigma}{\mu})$ becoming greater than 10 percent, the behavior turns non-linear.
4. The normalised characteristics of the plates is affected by the end conditions. The ply-orientation also affects the characteristics but its effect is quite small compared to the effect of end conditions.

5. With 20 percent of input SD the change in SD of normalised deflection characteristics is 23 percent for the SS plate and 24 percent for the CC plate.
6. The normalised characteristic curves of the plates with different ARs, boundary conditions, a/h and ply-orientations behave in a similar way and all of the curves fall within a tolerance of 1.5 percent of σ_{output} .
7. With one normalised behavioral curve, the displacement characteristics for a family of plates can be predicted. The actual displacement characteristics for these can be derived as the normalised factor is known.

Scope for future work

Having worked with this interesting problem for long the author would like to suggest the following for future work:

1. The effect of dispersion in the random material properties on the stresses and dynamics of the plate can be studied.
2. The random material properties were taken to have Normal distribution over lots and was assumed not to vary over the domain of the plate. The problem may be pursued with the material properties having different probability distributions over the domain of the plate as well as varying in lots.
3. The above problem can be pursued with random loading, plate geometry being circular, elliptical etc. The boundary condition may be fixed, SS, free and in combination at different edges. The parameters a/h , fiber orientation, etc. may be taken as random in nature.

References

- [1] S. Salim, "Analysis of composite plates with random material properties.," *Phd-Thesis Dept of Aerospace Engg., IIT Kanpur.*, April 1995.
- [2] R. A. Ibrahim, "Structural dynamics with parameter uncertainties," *Trans., ASME; Applied mechanics review*, vol. 40, no. 3, pp. 309–328, 1987.
- [3] S. Nakagiri, H. Takabatake, and S. Tani, "Uncertain eigen value analysis of composite laminated plates by the sfem," *Composite Structures*, vol. 109, pp. 9–12, 1987.
- [4] A. W. Leissa and A. F. Martin, "Vibration and buckling of rectangular composite plates with variable fiber spacing," *Composite Structures*, vol. 14, pp. 339–357, 1990.
- [5] S. P. Englestad and J. N. Reddy, "Probabilistic methods for the analysis of metal-matrix composite," *Composite Science and Technology*, vol. 50, pp. 91–107, 1994.
- [6] G. V. Vinckenroy and W. P. de Wilde, "The use of monte carlo techniques in sfem for determination of the structural behavior of composites," *Composite Structures*, vol. 32, pp. 247–253, 1995.
- [7] S. Salim, D. Yadav, and N. G. R. Iyengar, "Analysis of composite plates with random material characteristics.," *Mechanics Research Communication*, vol. 20, no. 5, pp. 405–414, 1993.

-
- [8] S. Salim, D. Yadav, and N. G. R. Iyengar, "Deflection of composite plates with random material characteristics.," *Proceedings of Int. Sym. on Aerospace Science and Engineering.*, pp. 236–239, Dec 12-15 1992.
- [9] S. Salim, D. Yadav, and N. G. R. Iyengar, "Free vibration of composite plates with randomness in material properties.," *Proceedings of the Fifth Intl. Conf. on Recent advances in Str. Dynamics*, pp. 814–823, July 18-21 1994.
- [10] P. C. Yang, C. H. Norris, and Y. Stavsky, "Elastic wave propagation in heterogeneous plates," *Int. J. Sol. Struct.*, vol. 2, pp. 665–684, 1966.
- [11] K. H. Lo, R. M. Christenson, and E. M. Wu, "A high-order theory of plate deformation," *Trans. ASME, J. Appl. Mech.*, vol. 44, pp. 663–668, 1977.
- [12] J. N. Reddy, "A simple higher order theory for laminated composite plates," *Trans. ASME, J. Appl. Mech.*, vol. 51, pp. 745–752, 1984.
- [13] C. A. Shankara, "Analysis of composite laminated plates subjected to mechanical, hygral and thermal loadings.," *Phd-Thesis Dept. of Aerospace Engg., IIT Kanpur.*, pp. 43–81, September 1993.
- [14] J. N. Reddy, "A refined non linear theory of plates with transverse shear deformation," *Int. J. Sol. Struct.*, vol. 20, pp. 881–896, 1984.